

1 TITLE

2 Identification of novel, clinically correlated autoantigens in the monogenic autoimmune syndrome
3 APS1 by PhIP-Seq

4

5 AUTHOR NAMES AND AFFILIATIONS

6 Sara E. Vazquez, AB, Department of Biochemistry and Biophysics, University of California, San
7 Francisco, CA, USA

8 Elise M. N. Ferré, PA-C, MPH, Fungal Pathogenesis Section, Laboratory of Clinical Immunology
9 and Microbiology, National Institute of Allergy and Infectious Diseases, National Institute of
10 Health, Bethesda, MD, USA

11 David W. Scheel, Diabetes Center, University of California, San Francisco, CA, USA

12 Sara Sunshine, BS, Department of Biochemistry and Biophysics, University of California, San
13 Francisco, CA, USA

14 Brenda Miao, BA, Diabetes Center, University of California, San Francisco, CA

15 Caleigh Mandel-Brehm, PhD, Department of Biochemistry and Biophysics, University of
16 California, San Francisco, CA, USA

17 Zoe Quandt, MD, MS, Department of Medicine, Division of Endocrinology, University of
18 California, San Francisco, CA, USA

19 Alice Y. Chan, MD, PhD, Department of Pediatrics, University of California, San Francisco, CA

20 Mickie Cheng, MD, PhD, Diabetes Center, University of California, San Francisco, CA, USA

21 Michael S. German, MD, Department of Medicine, Diabetes Center, and Eli and Edythe Broad
22 Center of Regeneration Medicine and Stem Cell Research, University of California San Francisco,
23 San Francisco, CA, USA

24 Michail S. Lionakis, MD, ScD, Fungal Pathogenesis Section, Laboratory of Clinical Immunology
25 and Microbiology, National Institute of Allergy & Infectious Diseases, National Institutes of
26 Health, Bethesda, MD, USA

27 Joseph L. DeRisi*, PhD, Department of Biochemistry and Biophysics, University of California,
28 San Francisco, and Chan Zuckerberg Biohub, San Francisco, CA, USA

29 Mark S. Anderson*, MD, PhD, Diabetes Center, University of California, San Francisco, CA,
30 USA

31

32 *these authors contributed equally

33

34 Address Correspondence to:

35 Mark S. Anderson, mark.anderson@ucsf.edu

36 or

37 Joseph L. DeRisi, joe@derisilab.ucsf.edu

38

39 ABSTRACT

40

41 The identification of autoantigens remains a critical challenge for understanding and treating
42 autoimmune diseases. Autoimmune polyendocrine syndrome type 1 (APS1), a rare monogenic
43 form of autoimmunity, presents as widespread autoimmunity with T and B cell responses to
44 multiple organs. Importantly, autoantibody discovery in APS1 can illuminate fundamental disease
45 pathogenesis, and many of the antigens found in APS1 extend to common autoimmune diseases.
46 Here, we performed proteome-wide programmable phage-display (PhIP-Seq) on sera from an
47 APS1 cohort and discovered multiple common antibody targets. These novel autoantigens exhibit
48 tissue-restricted expression, including expression in enteroendocrine cells and dental enamel.
49 Using detailed clinical phenotyping, we find novel associations between autoantibodies and organ-
50 restricted autoimmunity, including between anti-KHDC3L autoantibodies and premature ovarian
51 insufficiency, and between anti-RFX6 autoantibodies and diarrheal-type intestinal dysfunction.
52 Our study highlights the utility of PhIP-Seq for interrogating antigenic repertoires in human
53 autoimmunity and the importance of antigen discovery for improved understanding of disease
54 mechanisms.

55

56 INTRODUCTION

57 Autoimmune Polyglandular syndrome type 1 (APS1) or Autoimmune Polyglandular-
58 Candidiasis-Ectodermal Dystrophy (APECED; OMIM #240300) is an autoimmune syndrome
59 caused by monogenic mutations in the *AIRE* gene that result in defects in AIRE-dependent T cell
60 education in the thymus (Aaltonen et al., 1997; Anderson, 2002; Conteduca et al., 2018; Malchow
61 et al., 2016; Nagamine et al., 1997). As a result, people with APS1 develop autoimmunity to
62 multiple organs, including endocrine organs, skin, gut, and lung (Ahonen et al., 1990; Ferré et al.,
63 2016; Söderbergh et al., 2004). Although the majority of APS1 autoimmune manifestations are
64 thought to be primarily driven by autoreactive T cells, people with APS1 also possess autoreactive
65 B cells and corresponding high-affinity autoantibody responses (DeVoss et al., 2008; Gavanescu
66 et al., 2008; Meyer et al., 2016; Sng et al., 2019). These autoantibodies likely derive from germinal
67 center reactions driven by self-reactive T cells, resulting in mirroring of autoantigen identities
68 between the T and B cell compartments (Lanzavecchia, 1985; Meyer et al., 2016).

69 Identification of the specificity of autoantibodies in autoimmune diseases is important for
70 understanding underlying disease pathogenesis and for identifying those at risk for disease (Rosen
71 & Casciola-Rosen, 2014). However, despite the long-known association of autoantibodies with
72 specific diseases in both monogenic and sporadic autoimmunity, many autoantibody specificities
73 remain undiscovered. Challenges in antigen identification include the weak affinity of some
74 autoantibodies for their target antigen, as well as rare or low expression of the target antigen. One
75 approach to overcome some of these challenges is to interrogate autoimmune patient samples with
76 particularly high affinity autoantibodies. Indeed, such an approach identified GAD65 as a major
77 autoantigen in type 1 diabetes by using sera from people with Stiff Person Syndrome (OMIM
78 #184850), who harbor high affinity autoantibodies (Baekkeskov et al., 1990). We reasoned that

79 PhIP-Seq interrogation of APS1, a defined monogenic autoimmune syndrome with a broad
80 spectrum of high affinity autoantibodies, would likely yield clinically meaningful targets –
81 consistent with previously described APS1 autoantibody specificities that exhibit strong, clinically
82 useful associations with their respective organ-specific diseases (Alimohammadi et al., 2008,
83 2009; Ferré et al., 2019; Landegren et al., 2015; Popler et al., 2012; Puel et al., 2010; Shum et al.,
84 2013; Söderbergh et al., 2004; Winqvist et al., 1993).

85 The identification of key B cell autoantigens in APS1 has occurred most commonly
86 through candidate-based approaches and by whole-protein microarrays. For example, lung antigen
87 BPIFB1 autoantibodies, which are used to assess people with APS1 for risk of interstitial lung
88 disease, were discovered first in *Aire*-deficient mice using a combination of targeted
89 immunoblotting, tissue microscopy, and mass spectrometry (Shum et al., 2013, 2009). Recently,
90 there have been rapid advances in large platform approaches for antibody screening; these
91 platforms can overcome problems of antigen abundance by simultaneously screening the majority
92 of proteins from the human genome in an unbiased fashion (Jeong et al., 2012; Larman et al., 2011;
93 Sharon & Snyder, 2014; Zhu et al., 2001). In particular, a higher-throughput antibody target
94 profiling approach utilizing a fixed protein microarray technology (ProtoArray) has enabled
95 detection of a wider range of proteins targeted by autoantibodies directly from human serum
96 (Fishman et al., 2017; Landegren et al., 2016; Meyer et al., 2016). Despite initial success of this
97 technology in uncovering shared antigens across APS1 cohorts, it is likely that many shared
98 antigens remain to be discovered, given that these arrays do not encompass the full coding potential
99 of the proteome.

100 Here, we took an alternate approach to APS1 antigen discovery by employing Phage
101 Immunoprecipitation-Sequencing (PhIP-Seq) based on an established proteome-wide tiled library

102 (Larman et al., 2011; O'Donovan et al., 2018). This approach possesses many potential advantages
103 over previous candidate-based and whole-protein fixed array approaches, including (1) expanded,
104 proteome-wide coverage (including alternative splice forms) with 49 amino acid (AA) peptide
105 length and 24AA resolution tiling, (2) reduced volume requirement for human serum, and (3) high-
106 throughput, sequencing based output (Larman et al., 2011; O'Donovan et al., 2018). Of note, the
107 PhIP-Seq investigation of autoimmune diseases of the central nervous system, including
108 paraneoplastic disease, has yielded novel and specific biomarkers of disease (Larman et al., 2011;
109 Mandel-Brehm et al., 2019; O'Donovan et al., 2018).

110 Using a PhIP-Seq autoantibody survey, we identify a collection of novel APS1
111 autoantigens as well as numerous known, literature-reported APS1 autoantigens. We orthogonally
112 validate seven novel autoantigens including RFX6, KHDC3L, and ACP4, all of which exhibit
113 tissue-restricted expression (Jeong et al., 2012; Larman et al., 2011; Sharon & Snyder, 2014; H.
114 Zhu et al., 2001). Importantly, these novel autoantigens may carry important implications for
115 poorly understood clinical manifestations such as intestinal dysfunction, ovarian insufficiency, and
116 tooth enamel hypoplasia, where underlying cell-type specific antigens have remained elusive.
117 Together, our results demonstrate the applicability of PhIP-Seq to antigen discovery, substantially
118 expand the spectrum of known antibody targets and clinical associations in APS1, and point
119 towards novel specificities that can be targeted in autoimmunity.

120

121 RESULTS

122

123 **Investigation of APS1 serum autoantibodies by PhIP-Seq**

124 Individuals with APS1 develop autoantibodies to many known protein targets, some of
125 which exhibit tissue-restricted expression and have been shown to correlate with specific
126 autoimmune disease manifestations. However, the target proteins for many of the APS1 tissue-
127 specific manifestations remain enigmatic. To this end, we employed a high-throughput, proteome-
128 wide programmable phage display approach (PhIP-Seq) to query the antibody target identities
129 within serum of people with APS1 (Larman et al., 2011; O'Donovan et al., 2018). The PhIP-Seq
130 technique leverages large scale oligo production and efficient phage packaging and expression to
131 present a tiled-peptide representation of the proteome displayed on T7 phage. Here, we utilize a
132 phage library that we previously designed and deployed for investigating paraneoplastic
133 autoimmune encephalitis (Mandel-Brehm et al., 2019; O'Donovan et al., 2018). The library itself
134 contains approximately 700,000 unique phage, each displaying a 49 amino acid proteome segment.
135 As previously described, phage were immunoprecipitated using human antibodies bound to protein
136 A/G beads. In order to increase sensitivity and specificity for target proteins, eluted phage were
137 used for a further round of amplification and immunoprecipitation. DNA was then extracted from
138 the final phage elution, amplified and barcoded, and subjected to Next-Generation Sequencing
139 (**Figure 1A**). Finally, sequencing counts were normalized across samples to correct for variability
140 in sequencing depth, and the fold-change of each gene was calculated (comprised of multiple
141 unique tiling phage) as compared to mock IPs in the absence of human serum (further details of
142 the protocol can be found in the methods section).

143 From a cohort of 67 APS1 serum samples, a total of 39 samples were subjected to PhIP-
144 Seq investigation, while the remaining 28 samples were obtained at a later time point and reserved
145 for downstream validation experiments (for clinical data, refer to **Supplemental Table 1**). In
146 addition, 28 non-APS1 anonymous blood donor serum samples were subjected to PhIP-Seq, and
147 an additional group of 61 non-APS1 plasma samples were used for downstream validation
148 experiments.

149

150 **Detection of literature-reported APS1 autoantigens**

151 PhIP-Seq results were first cross-referenced with previously reported APS1 autoantibody
152 targets (Alimohammadi et al., 2008, 2009; Clemente et al., 1997; Fishman et al., 2017; Hedstrand
153 et al., 2001; Husebye et al., 1997; Kluger et al., 2015; Kuroda et al., 2005; Landegren et al., 2016,
154 2015; Leonard et al., 2017; Meager et al., 2006; Meyer et al., 2016; Oftedal et al., 2015; Pöntynen
155 et al., 2006; Sansom et al., 2014; Shum et al., 2013, 2009; Söderbergh et al., 2004). To avoid false
156 positives, a conservative set of criteria were used as follows. We required a minimum of 2/39
157 APS1 samples and 0/28 non-APS1 control samples to exhibit normalized gene counts in the
158 immunoprecipitation (IP) with greater than 10-fold enrichment as compared to the control set of
159 18 mock-IP (beads, no serum) samples. This simple, yet stringent criteria enabled detection of a
160 total of 23 known autoantibody specificities (**Figure 1B**). Importantly, many of the well-validated
161 APS1 antigens, including specific members of the cytochrome P450 family (CYP1A2, CYP21A1,
162 CYP11A1, CYP17A1), lung disease-associated antigen KCRNG, as well as IL17A, IL17F, and
163 IL22, among others were well represented (**Figure 1B**). In contrast, the diabetes-associated
164 antigens GAD65 and INS did not meet these stringent detection criteria and only weak signal was
165 detected to many of the known interferon autoantibody targets known to be present in many people

166 with APS1, perhaps due to the conformational nature of these autoantigens (**Figure 1B & Figure**
167 **1: Figure Supplement 1**) (Björk et al., 1994; Meager et al., 2006; Meyer et al., 2016; Wolff et al.,
168 2013; Ziegler et al., 1996).

169 Three known autoantigens that were prevalent within our cohort were selected to determine
170 how PhIP-Seq performed against an orthogonal whole protein-based antibody detection assay. A
171 radioligand binding assay (RLBA) was performed by immunoprecipitating *in vitro* transcribed and
172 translated S35-labeled proteins CYP11A1, SOX10, and NLRP5 with APS1 serum
173 (Alimohammadi et al., 2008; Berson et al., 1956; Hedstrand et al., 2001; Winqvist et al., 1993).
174 Importantly, and in contrast to PhIP-Seq, this assay tests for antibody binding to full-length protein
175 (**Figure 1C**). By RLBA, these three antigens were present in and specific to both the initial
176 discovery APS1 cohort (n=39) as well as the expanded validation cohort (n = 28), but not the non-
177 APS1 control cohort (n = 61). Together, these results demonstrate that PhIP-Seq detects known
178 APS1 autoantigens and that PhIP-Seq results validate well in orthogonal whole protein-based
179 assays.

180 To determine whether the PhIP-Seq APS1 dataset could yield higher resolution information
181 on antigenic peptide sequences with respect to previously reported targets, the normalized
182 enrichments of all peptides belonging to known disease-associated antigens CYP11A1 and SOX10
183 were mapped across the full length of their respective proteins (**Figure 1: Figure Supplement 2**).
184 The antigenic regions within these proteins were observed to be similar across all samples positive
185 for anti-CYP11A1 and anti-SOX10 antibodies, respectively (**Figure 1: Figure Supplement 2**)
186 suggesting peptide-level commonalities and convergence among the autoreactive antibody
187 repertoires across individuals. These data suggest that people with APS1 often target similar, but
188 not identical protein regions.

189

190 **Identification of novel APS1 autoantigens**

191 Having confirmed that PhIP-Seq analysis of APS1 sera detected known antigens, the same
192 data were then investigated for the presence of novel, previously uncharacterized APS1
193 autoantigens. We applied the same positive hit criteria as described for known antigens, and
194 additionally increased the required number of positive APS1 samples to 3/39 to impose a stricter
195 limit on the number of novel candidate autoantigens. This yielded a list of 82 genes, which included
196 10 known antigens and 72 putative novel antigens (**Figure 2**).

197 The most commonly held hypotheses regarding the nature and identity of proteins targeted
198 by the aberrant immune response in APS1 are that targeted proteins (1) tend to exhibit AIRE-
199 dependent thymic expression and (2) have restricted expression to one or few peripheral organs
200 and tend not to be widely or ubiquitously expressed. We investigated whether our novel antigens
201 were also preferentially tissue-restricted. In order to systematically address this question, tissue-
202 specific RNA expression was assessed using a consensus expression dataset across 74 cell types
203 and tissues (Uhlen et al., 2015). For each gene, the ratio of expression in the highest tissue as
204 compared to the sum of expression across all tissues was calculated, resulting in higher ratios for
205 those mRNAs with greater degrees of tissue-restriction. Using this approach, the mean tissue-
206 specificity ratio of the 82 PhIP-Seq positive antigens was increased by approximately 1.5-fold
207 ($p=0.0017$) as compared to the means from iterative sampling of 82 genes (**Figure 2: Figure**
208 **Supplement 1**).

209

210 **Identification of novel antigens common to many individuals**

211 Identified autoantigens were ranked by frequency within the cohort. Five antigens were
212 positive in ten or more APS1 samples, including two novel antigens. In addition, the majority of
213 antigens found in 4 or more APS1 sera were novel (**Figure 3A**). Five of the most frequent novel
214 antigens were selected for subsequent validation and follow-up. These included RFX6, a
215 transcription factor implicated in pancreatic and intestinal pathology (Patel et al., 2017; S. B. Smith
216 et al., 2010); ACP4, an enzyme implicated in dental enamel hypoplasia (Choi et al., 2016; Seymen
217 et al., 2016; C. E. Smith et al., 2017); KHDC3L, a protein with oocyte-restricted expression (Li et
218 al., 2008; Zhang et al., 2018; K. Zhu et al., 2015); NKX6-3, a gastrointestinal transcription factor
219 (Alanentalo et al., 2006); and GIP, a gastrointestinal peptide involved in intestinal motility and
220 energy homeostasis (Adriaenssens et al., 2019; Moody et al., 1984; Pederson & McIntosh, 2016).
221 Several less frequent (but still shared) novel antigens were also chosen for validation, including
222 ASMT, a pineal gland enzyme involved in melatonin synthesis (Ackermann et al., 2006; Rath et
223 al., 2016); and PDX1, an intestinal and pancreatic transcription factor (Holland et al., 2002;
224 Stoffers et al., 1997) (**Figure 3A**). Of note, this group of seven novel antigens all exhibited either
225 tissue enriched, tissue enhanced, or group enhanced expression according to the Human Protein
226 Atlas database (Uhlen et al., 2015) (**Supplemental Table 2**). Using a whole-protein radiolabeled
227 binding assay (RLBA) for validation, all seven proteins were immunoprecipitated by antibodies in
228 both the PhIP-Seq APS1 discovery cohort (n=39), as well as in the validation cohort of APS1 sera
229 that had not been interrogated by PhIP-Seq (n=28). Whereas an expanded set of non-APS1 controls
230 (n=61) produced little to no immunoprecipitation signal by RLBA as compared to positive control
231 antibodies (low antibody index), APS1 samples yielded significant immunoprecipitation signal
232 enrichment for each whole protein assay (high antibody index) (**Figure 3B & Supplemental**
233 **Table 3**).

234 The comparison of PhIP-Seq data to the results from the RLBA (n=39, discovery cohort
235 only) yielded positive correlations between the two datasets ($r = 0.62-0.95$; **Figure 3: Figure**
236 **Supplement 1**). Notably, for some antigens, such as NLRP5, and particularly for ASMT, the
237 RLBA results revealed additional autoantibody-positive samples not detected by PhIP-Seq
238 (**Figure 3B & Figure 3: Figure Supplement 1 & Figure 1: Figure Supplement 2**).

239

240 **Autoantibody-disease associations for both known and novel antigens**

241 Because the individuals in this APS1 cohort have been extensively phenotyped for 24
242 clinical manifestations, the PhIP-Seq APS1 data was queried for phenotypic associations. Several
243 autoantibody specificities, both known and novel, were found to possess highly significant
244 associations with several clinical phenotypes (**Figure 4 & Figure 4: Figure Supplement 1**).
245 Among these were the associations of KHDC3L with ovarian insufficiency, RFX6 with diarrheal-
246 type intestinal dysfunction, CYP11A1 (also known as cholesterol side chain cleavage enzyme)
247 with adrenal insufficiency (AI), and SOX10 with vitiligo (**Figure 4**). Strikingly, anti-CYP11A1
248 antibodies are present in AI and are known to predict disease development (Betterle et al., 2002;
249 Obermayer-Straub et al., 2000; Winqvist et al., 1993). Similarly, antibodies to SOX10, a
250 transcription factor involved in melanocyte differentiation and maintenance, have been previously
251 shown to correlate with the presence of autoimmune vitiligo (Hedstrand et al., 2001).

252

253 **Anti-KHDC3L antibodies in APS1-associated ovarian insufficiency**

254 Primary ovarian insufficiency is a highly penetrant phenotype, with an estimated 60% of
255 females with APS1 progressing to an early, menopause-like state (Ahonen et al., 1990; Ferré et
256 al., 2016). Interestingly, a set of 5 proteins (KHDC3L, SRSF8, PNO1, RASIP1, and MORC2)

257 exhibited a significant association with ovarian insufficiency in this cohort (**Figure 4**). A publicly
258 available RNA-sequencing dataset from human oocytes and supporting granulosa cells of the
259 ovary confirmed that of these 5 genes, only *KHDC3L* exhibited expression levels in female oocytes
260 comparable to the expression levels seen for the known oocyte markers *NLRP5* and *DDX4* (Zhang
261 et al., 2018) (**Figure 4: Figure Supplement 2**). We therefore chose to further investigate the
262 relationship between anti-KHDC3L antibodies and ovarian insufficiency in our cohort (**Figure 5**).

263 *KHDC3L* is a well-studied molecular binding partner of *NLRP5* within the ovary (Li et al.,
264 2008; K. Zhu et al., 2015). Together, *NLRP5* and *KHDC3L* form part of a critical oocyte-specific
265 molecular complex, termed the subcortical maternal complex (SCMC) (Bebbere et al., 2016;
266 Brozzetti et al., 2015; Li et al., 2008; Liu et al., 2016; K. Zhu et al., 2015). Furthermore, knockout
267 of the *NLRP5* and *KHDC3L* in female mice results in fertility defects, and human genetic mutations
268 in these genes of the SCMC have been linked to infertility and molar pregnancies (Li et al., 2008;
269 Y. Zhang et al., 2018; K. Zhu et al., 2015). Interestingly, previous work established *NLRP5* as a
270 parathyroid-specific antigen in APS1, with potential for additional correlation with ovarian
271 insufficiency (Alimohammadi et al., 2008). However, anti-*NLRP5* antibodies lack sensitivity for
272 ovarian insufficiency. Importantly, unlike *NLRP5*, *KHDC3L* is expressed primarily in the ovary,
273 and thus potentially represents a more oocyte-specific autoantigen (Liu et al., 2016; Virant-Klun
274 et al., 2016; Y. Zhang et al., 2018). Using the dataset from Zhang et. al, we confirmed that
275 *KHDC3L*, as well as *NLRP5* and the known oocyte marker *DDX4*, are highly expressed within
276 the oocyte population, but not in the supporting granulosa cell types (Y. Zhang et al., 2018) (**Figure**
277 **5A**). Interestingly, the majority (64%) of APS1 sera had a concordant status for antibodies to
278 *KHDC3L* and *NLRP5* (**Figure 5B**). Although previous reports did not find a strong gender
279 prevalence within samples positive for anti-*NLRP5* antibodies, the mean anti-*NLRP5* and anti-

280 KHDC3L antibody signals were increased in females in this cohort (**by 1.6- and 2.1-fold,**
281 **respectively; Figure 5C**). Finally, all 10 females in the expanded APS1 cohort with diagnosed
282 ovarian insufficiency were also positive for anti-KHDC3L antibodies (**Figure 5D**).

283

284 **High prevalence of anti-ACP4 antibodies**

285 Similar to known antigens CYP11A1, SOX10, and LCN1, the novel antigen ACP4 was
286 found to occur at high frequencies in this cohort (**Figure 3A**). ACP4 (acid phosphatase 4) is highly
287 expressed in dental enamel, and familial mutations in the *ACP4* gene result in dental enamel
288 hypoplasia similar to the enamel hypoplasia seen in ~90% of this APS1 cohort (Seymen et al.,
289 2016; C. E. Smith et al., 2017). Strikingly, 50% of samples were positive for anti-ACP4 antibodies
290 by RLBA, with excellent correlation between RLBA and PhIP-Seq data (**Figure 3B & Figure 3:**
291 **Figure Supplement 1A**). Consistently, samples from individuals with enamel hypoplasia
292 exhibited a trend towards higher anti-ACP4 antibody signal by RLBA (**Figure 3: Figure**
293 **Supplement 1B, p = 0.064**).

294

295 **High prevalence of anti-RFX6 antibodies**

296 In this cohort, 82% (55/67) of APS1 sera exhibited an RFX6 signal that was at least 3
297 standard deviations above the mean of non-APS1 control signal due to the extremely low RFX6
298 signal across all non-APS1 controls by RLBA (**Figure 3B**). Using a more stringent cutoff for
299 RFX6 positivity by RLBA at 6 standard deviations above the mean, 65% of APS1 samples were
300 positive for anti-RFX6 antibodies. RFX6 is expressed in both intestine and pancreas, and loss of
301 function RFX6 variants in humans lead to both intestinal and pancreatic pathology (Gehart et al.,
302 2019; Patel et al., 2017; Piccand et al., 2019; S. B. Smith et al., 2010). Interestingly, across all

303 samples with anti-RFX6 antibodies, the response targeted multiple sites within the protein,
304 suggesting a polyclonal antibody response (**Figure 6: Figure Supplement 1A**).

305

306 **Anti-enteroendocrine and anti-RFX6 response in APS1**

307 The extent and frequency of intestinal dysfunction in people with APS1 has only recently
308 been clinically uncovered and reported, and therefore still lacks unifying diagnostic markers as
309 well as specific intestinal target antigen identities (Ferré et al., 2016). This investigation of APS1
310 sera revealed several antigens that are expressed in the intestine, including RFX6, GIP, PDX1, and
311 NKX6-3. We chose to further study whether autoimmune response to RFX6+ cells in the intestine
312 was involved in APS1-associated intestinal dysfunction. Using a publicly available murine single-
313 cell RNA sequencing dataset of 16 different organs and over 120 different cell types, *RFX6*
314 expression was confirmed to be present in and restricted to pancreatic islets and intestinal
315 enteroendocrine cells (Schaum et al., 2018) (**Figure 6: Figure Supplement 1B & 1C**). Serum
316 from an individual with APS1-associated intestinal dysfunction and anti-RFX6 antibodies was
317 next tested for reactivity against human intestinal enteroendocrine cells, revealing strong nuclear
318 staining that colocalized with ChromograninA (ChgA), a well-characterized marker of intestinal
319 enteroendocrine cells (Goldspink et al., 2018; O'Connor et al., 1983) (**Figure 6A, right panel and**
320 **inset**). In contrast, enteroendocrine cell staining was not observed from APS1 samples that lacked
321 anti-RFX6 antibodies or from non-APS1 control samples. (**Figure 6A, center & left panels**).
322 Furthermore, serum from samples with anti-RFX6 antibodies stained transfected tissue culture
323 cells expressing RFX6 (**Figure 6B, Figure 6: Figure Supplement 2**). These data support the
324 notion that there exists a specific antibody signature, typified by anti-RFX6 antibodies, associated
325 with enteroendocrine cells in APS1.

326 Both mice and humans with biallelic mutation of the gene encoding RFX6 have
327 enteroendocrine cell deficiency and intestinal malabsorption (Mitchell et al., 2004; Piccand et al.,
328 2019; S. B. Smith et al., 2010), and humans with other forms of genetic or acquired
329 enteroendocrine cell deficiency also suffer from chronic malabsorptive diarrhea (Akoury et al.,
330 2015; Li et al., 2008; Reddy et al., 2012; X. Wang et al., 2018; W. Zhang et al., 2019). In this
331 cohort, 54/67 (81%) of individuals have intestinal dysfunction defined as the presence of chronic
332 diarrhea, chronic constipation or an alternating pattern of both, without meeting ROME III
333 diagnostic criteria for irritable bowel syndrome, as previously described (Ferré et al., 2016). When
334 the cohort was subsetted by presence or absence of intestinal dysfunction, the anti-RFX6 RLBA
335 signal was significantly higher when intestinal dysfunction was present (**Figure 6C**). Further
336 subsetting of the cohort by subtype of intestinal dysfunction revealed that individuals with anti-
337 RFX6 antibodies belonged preferentially to the diarrheal-type (as opposed to constipation-type)
338 group of intestinal dysfunction (**Figure 6D & Figure 6: Figure Supplement 3A**). Given that
339 RFX6 is also expressed in the pancreas, we also examined the association of anti-RFX6 antibodies
340 with APS1-associated type 1 diabetes. We observed that 6/7 APS1-associated type 1 diabetes
341 samples had positive signal for anti-RFX6 antibodies by RLBA (**Figure 6: Figure Supplement**
342 **3B**). However, due to small sample size, an expanded cohort would be needed to determine the
343 significance of this observation. Together, these data suggest that RFX6 is a common, shared
344 autoantigen in APS1 that may be involved in the immune response to intestinal enteroendocrine
345 cells as well as pancreatic islets. Future studies will help to determine whether testing for anti-
346 RFX6 antibodies possesses clinical utility for prediction or diagnosis of specific APS1
347 autoimmune disease manifestations as well as for non-APS1 autoimmune disease.
348

349 DISCUSSION

350

351 Here, we have identified a new set of autoantigens that are associated with autoimmune
352 features in APS1 by using the broad-based antigen screening platform of PhIP-Seq. Unlike fixed
353 protein arrays, programmable phage display possesses the advantage of being able to
354 comprehensively cover all annotated proteins and their isoforms. The PhIP-Seq library used here
355 is composed of over 700,000 peptides, each 49 amino acids, and corresponding to approximately
356 20,000 proteins and their known splicing isoforms. This is highly complementary to recently
357 published protein arrays that cover approximately 9,000 distinct proteins (Fishman et al., 2017;
358 Landegren et al., 2016; Meyer et al., 2016). Recent protein array approaches with APS1 samples
359 using strict cutoffs have been able to identify a number of new autoantigen targets that include
360 PDILT and MAGEB2 (Landegren et al., 2016). Several new targets, including RFX6, KHDC3L,
361 ACP4, NKX6-3, ASMT, and PDX1, were likely discovered here because these antigens were not
362 present on previously published protein array platforms. Only a subset of the novel targets
363 identified here were validated orthogonally. While none failed validation relative to non-APS1
364 controls, further validation work will be needed for the many additional novel targets identified by
365 PhIP-Seq. It is also worth mentioning that the PhIP-Seq method leverages continuing declines in
366 the cost of oligonucleotide synthesis and Next-Generation Sequencing. Both technologies benefit
367 from economies of scale, and once constructed, a PhIP-Seq phage library may be propagated in
368 large quantities at negligible cost. The primary disadvantage of PhIP-Seq is the fact that
369 conformation specific antibodies are likely to be missed, unless short linear subsequences carry
370 significant binding energy. For example, PhIP-Seq detected only limited signal towards some
371 literature reported antigens, including GAD65 and interferon family proteins in this APS1 cohort.

372 Given that these antigens have been reported to involve conformational epitopes, antibodies to
373 these antigens would not be predicted to be easily detected by linear peptides (Björk et al., 1994;
374 Meager et al., 2006; Meyer et al., 2016; Wolff et al., 2013; Ziegler et al., 1996). Nonetheless, the
375 ability to detect anti-interferon antibodies in a subset of APS1 samples highlights the utility of
376 PhIP-Seq for antigen discovery despite decreased sensitivity for certain epitopes (**Figure 1: Figure**
377 **Supplement 1**).

378 People with (Anderson, 2002; Cheng & Anderson, 2018; Husebye et al., 2018; Malchow
379 et al., 2016)APS1 develop autoimmune manifestations over the course of many years, and it is
380 thought that each manifestation may be explained by autoimmune response to one or few initial
381 protein targets. In principle, these target proteins would most likely (1) exhibit thymic AIRE-
382 dependency and (2) be restricted to the single or narrow range of tissues associated with the
383 corresponding autoimmune disease. For example, adrenal insufficiency, which results from
384 autoimmune response to cells of the adrenal gland, is thought to occur due to targeting of adrenally-
385 expressed cytochrome p450 family members (Obermayer-Straub et al., 2000; Winqvist et al.,
386 1993). However, a more complete understanding of the protein target spectrum paired with clinical
387 phenotypic associations has been lacking. This, combined with the limited applicability of murine
388 observations to the human disease, has left the question of which clinical characteristics best
389 associate with APS1 autoantigens a heavily debated subject (Pöntynen et al., 2006).

390 Testing for defined autoantibody specificities provides substantial clinical benefit for
391 prediction and diagnosis of autoimmune disease. A primary goal of this study was to identify
392 autoantigens with potential clinical significance; consistently, our analyses focused primarily on
393 antigens that appeared across multiple samples, rather than autoantigens that were restricted to
394 individual samples. Using conservative inclusion criteria, we discovered 72 novel autoantigens

395 that were shared across a minimum of 3 APS1 samples, of which 7/7 were successfully validated
396 at the whole protein level. Overall, we have expanded the known repertoire of common APS1
397 antigens, confirming that the antibody target repertoire of common antigens in APS1 is larger than
398 previously appreciated. Interestingly, our data also suggest that the size of the commonly
399 autoantibody-targeted repertoire of proteins is dramatically lower than the number of genes
400 (~4000) that exhibit AIRE-dependent thymic expression.

401 The spectrum of different autoimmune diseases that can be observed in APS1 is extensive
402 and has continued to expand through investigation of larger cohorts (Ahonen et al., 1990; Bruserud
403 et al., 2016; Ferré et al., 2016). In this study, clinical metadata encompassing disease status across
404 24 individual disease manifestations in a total of 67 people with APS1 was leveraged to uncover
405 (among others) an association of anti-KHDC3L antibodies and ovarian insufficiency, a disease
406 that affects over half of all women with APS1 and manifests as abnormal menstrual cycling,
407 reduced fertility, and early menopause. While autoreactivity to the steroidogenic granulosa cells –
408 the cells surrounding and supporting the oocytes – has been proposed as one etiology of the clinical
409 ovarian insufficiency, it has also been suggested that there may exist an autoimmune response to
410 the oocyte itself (Jasti et al., 2012; Maclaren et al., 2001; Obermayer-Straub et al., 2000; Otsuka
411 et al., 2011; Welt, 2008). Our finding that females with APS1-associated ovarian insufficiency
412 exhibit autoantibodies to KHDC3L, an oocyte specific protein, supports this hypothesis. As
413 exemplified by autoantibody presence in other autoimmune conditions, anti-KHDC3L antibodies
414 may also have predictive value. Specifically, in our cohort, we found anti-KHDC3L antibodies to
415 be present in many young, pre-menstrual females; these observations will require additional
416 studies in prospective, longitudinal cohorts for further evaluation of potential predictive value.
417 Interestingly, primary ovarian insufficiency (POI) in the absence of AIRE-deficiency is

418 increasingly common and affects an estimated 1 in 100 women; up to half of these cases have been
419 proposed to have autoimmune etiology (Huhtaniemi et al., 2018; Jasti et al., 2012; Nelson, 2009;
420 Silva et al., 2014).

421 We noted that the majority of samples with antibodies to KHDC3L also exhibited
422 antibodies to NLRP5, and vice versa. Remarkably, both of these proteins are critical parts of a
423 subcortical maternal complex (SCMC) in both human and murine oocytes (Li et al., 2008; K. Zhu
424 et al., 2015). Indeed, “multi-pronged” targeting of the same pathway has been previously
425 implicated in APS1, where antibodies to DDC and TPH1 – enzymes in the serotonin and melatonin
426 synthesis pathways – have been described (Ekwall et al., 1998; Husebye et al., 1997; Kluger et al.,
427 2015). In addition to these targets, our data revealed an additional autoantibody-targeted enzyme
428 ASMT in the same melatonin synthesis pathway. While the earlier TPH1- and DDC-catalyzed
429 steps occur in both the intestine and pineal gland and precede the formation of serotonin, ASMT
430 is predominantly expressed in the pineal gland and catalyzes the last, post-serotonin step in
431 melatonin synthesis, suggesting that targeting of this pathway occurs at multiple distinct steps. To
432 our knowledge, this is the first reported autoantigen in APS1 whose expression is restricted to the
433 central nervous system.

434 In past and ongoing investigations, some individuals with APS1 have been reported to
435 feature histologic loss of intestinal enteroendocrine cells on biopsy (Högenauer et al., 2001; Oliva-
436 Hemker et al., 2006; Posovszky et al., 2012, Natarajan et al., manuscript in preparation). The
437 association of anti-RFX6 antibodies with the diarrheal type of intestinal dysfunction is consistent
438 with published studies in murine models of *Rfx6* (and enteroendocrine cell) ablation (Piccand et
439 al., 2019; S. B. Smith et al., 2010). In addition, human enteroendocrine cell deficiency as well as
440 mutations in enteroendocrine gene *NEUROG3* have been linked to chronic diarrhea and

441 malabsorption, and recently, intestinal enteroendocrine cells have been suggested to play a role in
442 mediating intestinal immune tolerance (Ohsie et al., 2009; Sifuentes-Dominguez et al., 2019; J.
443 Wang et al., 2006). In sum, although APS1-associated intestinal dysfunction may have multiple
444 etiologies, including autoimmune enteritis or dysfunction of exocrine pancreas, our findings of
445 highly prevalent anti-RFX6 antibodies provide evidence of a common, shared autoantigen
446 involved with this disease phenotype. In addition, patients with type 1 diabetes alone (not in
447 association with APS1) frequently exhibit intestinal dysfunction related to multiple etiologies
448 including Celiac disease, autonomic neuropathy, and exocrine pancreatic insufficiency (Du et al.,
449 2018); future studies will be needed to determine whether anti-RFX6 antibodies may distinguish
450 a subset of these patients with an autoimmune enteroendocrinopathy contributing to their
451 symptoms.

452 While we report many novel antigens, we also acknowledge that the relationship between
453 autoantibody status and disease is often complicated. This concept can be illustrated by examining
454 the well-established autoantibody specificities in autoimmune diabetes (Taplin & Barker, 2009).
455 First, islet autoantibodies (GAD65, ZNT8, etc.) can be found within non-autoimmune sera, where
456 they are thought to represent an increased risk of developing disease as compared to the antibody-
457 negative population. Second, not all patients with autoimmune diabetes are autoantibody positive.
458 In sum, while autoantibodies can be extremely useful for risk assessment as well as for diagnosis,
459 they often lack high sensitivity and specificity; both of these caveats can result in difficulties
460 detecting strong clinical associations. For example, anti-ACP4 antibodies are highly prevalent in
461 our cohort, but they exhibit only a trending association with dental enamel hypoplasia despite the
462 strong biological evidence that ACP4 dysfunction leads to enamel hypoplasia (Seymen et al., 2016;
463 C. E. Smith et al., 2017). Our data in humans is currently insufficient to determine whether immune

464 responses to novel antigens such as ACP4 are pathogenic, indirectly linked to risk of disease, or
465 instead simply represent a B-cell bystander effect. To better address these questions, we propose
466 that future studies in mouse models could elucidate whether immune response to specific proteins,
467 including ACP4, can result in the proposed phenotypes.

468 As the spectrum of diseases with potential autoimmune etiology continues to expand, the
469 characteristic multiorgan autoimmunity in APS1 provides an ideal model system to more broadly
470 approach the question of which proteins and cell types tend to be aberrantly targeted by the immune
471 system. The data presented here has illuminated a collection of novel human APS1 autoimmune
472 targets, as well as a novel antibody-disease association between RFX6 and diarrheal-type intestinal
473 dysfunction, a highly prevalent disorder in APS1 that has until now lacked clinically applicable
474 predictive or diagnostic markers. In sum, this data has significantly expanded the known
475 autoantigen target profile in APS1 and highlighted several new directions for exploring the
476 mechanics and clinical consequences of this complex syndrome.

477 MATERIALS AND METHODS

478

479 Data collection

480 All patient cohort data was collected and evaluated at the NIH, and all APECED/APS1 patients
481 were enrolled in a research study protocols approved by the NIAID, NIH Clinical Center, and NCI
482 Institutional Review Board Committee and provided with written informed consent for study
483 participation. All NIH patients gave consent for passive use of their medical record for research
484 purposes (protocol #11-I-0187). The majority of this cohort data was previously published by Ferré
485 et al. 2016 and Ferré et al. 2019.

486

487 Phage Immunoprecipitation – Sequencing (PhIP-Seq)

488 For PhIP-Seq, we adapted a custom-designed phage library consisting of 731,724 49AA
489 peptides tiling the full protein-coding human genome including all isoforms (as of 2016) with
490 25AA overlap as previously described (O'Donovan et al., 2018). 1 milliliter of phage library was
491 incubated with 1 microliter of human serum overnight at 4C, and human antibody (bound to phage)
492 was immunoprecipitated using 40ul of a 1:1 mix of protein A/G magnetic beads (Thermo Fisher,
493 Waltham, MA, #10008D & #10009D). Beads were washed 4 times and antibody-bound phage
494 were eluted into 1ml of E. Coli at OD of 0.5-0.7 (BLT5403, EMD Millipore, Burlington, MA) for
495 selective amplification of eluted phage. This library was re-incubated with human serum and
496 repeated, followed by phenol-chloroform extraction of DNA from the final phage library. DNA
497 was barcoded and amplified (Phusion PCR, 30 rounds), gel purified, and subjected to Next-
498 Generation Sequencing on an Illumina MiSeq Instrument (Illumina, San Diego, CA).

499

500

501 PhIP-Seq Analysis

502 Sequencing reads from fastq files were aligned to the reference oligonucleotide library and peptide
503 counts were subsequently normalized by converting raw reads to percentage of total reads per
504 sample. Peptide and gene-level enrichments for both APS1 and non-APS1 sera were calculated by
505 determining the fold-change of read percentage per peptide and gene in each sample over the mean
506 read percentage per peptide and gene in a background of mock-IP (A/G bead only, n = 18).
507 Individual samples were considered positive for genes where the enrichment value was 10-fold or
508 greater as compared to mock-IP. For plotting of multiple genes in parallel (**Figures 1 & 2**),
509 enrichment values were z-scored and hierarchically clustered using Pearson correlation.

510

511 Statistics

512 For comparison of distribution of PhIP-Seq gene enrichment between APS1 patients with and
513 without specific disease manifestations, a (non-parametric) Kolmogorov-Smirnov test was used.
514 For radioligand binding assays, antibody index for each sample was calculated as follows: (sample
515 value – mean blank value) / (positive control antibody value – mean blank value). Comparison of
516 antibody index values between non-APS1 control samples and APS1 samples was performed using
517 a Mann-Whitney *U* test. Experimental samples that fell 3 standard deviations above of the mean
518 of non-APS1 controls for each assay were considered positive, except in the case of RFX6, where
519 a cutoff of 6 standard deviations above the mean of non-APS1 controls was used.

520

521 Assessing tissue-specific RNA expression

522 To determine tissue-specificity and tissue-restriction of *Rfx6* expression in mice, we used publicly
523 available Tabula Muris data (tabula-muris.ds.czbiohub.org) (Schaum et al., 2018). For
524 investigation of *KHDC3L* expression in human ovary, we downloaded publicly available
525 normalized FPKM transcriptome data from human oocytes and granulosa cells
526 (GSE107746_Folliculogenesis_FPKM.log2.txt) (Y. Zhang et al., 2018). With this data, we
527 performed principle component analysis, which clustered the two cell types correctly according to
528 their corresponding sample label, and plotted log₂(FPKM) by color for each sample.

529

530 293T overexpression assays

531 Human kidney embryo 293T (ATCC, Manassas, VA, #CRL-3216) cells were plated at 30%
532 density in a standard 24-well glass bottom plate in complete DMEM media (Thermo Fisher,
533 #119651198) with 10% Fetal Bovine Serum (Thermo Fisher, #10438026), 292ug/ml L-glutamine,
534 100ug/ml Streptomycin Sulfate, and 120Units/ml of Penicillin G Sodium (Thermo Fisher,
535 #10378016). 18 hours later, cells were transiently transfected using a standard calcium chloride
536 transfection protocol. For transfections, 0.1ug of sequence-verified pCMV-insert-MYC-FLAG
537 overexpression vectors containing either no insert (Origene #PS100001; ‘mock’ transfection) or
538 RFX6 insert (Origene #RC206174) were transfected into each well. 24 hours post-transfection,
539 cells were washed in 1X PBS and fixed in 4% PFA for 10 minutes at room temperature.

540

541 293T indirect immunofluorescence

542 Fixed 293T cells were blocked for 1 hour at room temperature in 5% BSA in PBST. For primary
543 antibody incubation, cells were incubated with human serum (1:1000) and rabbit anti-FLAG
544 antibody (1:2000) in 5% BSA in PBST for 2 hours at room temperature (RT). Cells were washed

545 4X in PBST and subsequently incubated with secondary antibodies (goat anti-rabbit IgG 488,
546 Invitrogen, Carlsbad, CA; #A-11034, 1:4000; & goat anti-human 647, Invitrogen #A-21445,
547 1:4000) for 1 hour at room temperature. Finally, cells were washed 4X in PBST, incubated with
548 DAPI for 5 minutes at RT, and subsequently placed into PBS for immediate imaging. All images
549 were acquired with a Nikon Ti inverted fluorescence microscope (Nikon Instruments, Melville,
550 NY). All experiments were performed in biological duplicates.

551

552 Indirect dual immunofluorescence on human fetal intestine

553 Human fetal small bowels (21.2 days gestational age) were processed as previously described
554 (Berger et al., 2015). Individual APS1 sera (1:4000 dilution) were used in combination with rabbit
555 antibodies to human Chromogranin A (Abcam, Cambridge, MA; #ab15160, 1:5000 dilution).
556 Immunofluorescence detection utilized secondary Alexa Fluor secondary antibodies (Life
557 Technologies, Waltham, MA; 488 goat anti-human IgG, #A11013; & 546 goat anti-rabbit IgG,
558 #A11010). Nuclear DNA was stained with Hoechst dye (Invitrogen, #33342). All images were
559 acquired with a Leica SP5 White Light confocal laser microscope (Leica Microsystems, Buffalo
560 Grove, IL).

561

562 ³⁵S-radiolabeled protein generation and binding assay

563 DNA plasmids containing full-length cDNA under the control of a T7 promoter for each of the
564 validated antigens (**Supplemental Table 3**) were verified by Sanger sequencing and used as DNA
565 templates in the T7 TNT in vitro transcription/translation kit (Promega, Madison, WI; #L1170)
566 using [³⁵S]-methionine (PerkinElmer, Waltham, MA; #NEG709A). Protein was column-purified
567 on Nap-5 columns (GE healthcare, Chicago, IL; #17-0853-01) and immunoprecipitated on

568 Sephadex protein A/G beads (Sigma Aldrich, St. Louis, MO; #GE17-5280-02 and #GE17-0618-
569 05, 4:1 ratio) in duplicate with serum or control antibodies in 96-well polyvinylidene difluoride
570 filtration plates (Corning, Corning, NY; #EK-680860). Each well contained 35'000 counts per
571 minute (cpm) of radiolabeled protein and 2.5ul of serum or appropriately diluted control antibody
572 **(Supplemental Table 3)**. The cpms of immunoprecipitated protein was quantified using a 96-well
573 Microbeta Trilux liquid scintillation plate reader (Perkin Elmer).

574

575

576 ACKNOWLEDGEMENTS

577 We thank Joseph M. Repogle, Jeffrey A. Hussmann, Madhura Raghavan, Hanna Retallack, Brian
578 D. O'Donovan, and members of the DeRisi, Anderson, Lionakis, and German labs for helpful
579 discussions. We thank Kari Herrington and the UCSF Nikon Imaging Center for imaging support,
580 as well as Sabrina Mann, Wint Lwin, and the UCSF Center for Advanced Technology for technical
581 support. We thank the New York Blood Bank for providing us with the de-identified human non-
582 inflammatory control plasma samples used in this study.

583 COMPETING INTERESTS

584 JD is a scientific advisory board member of Allen and Company. MSA owns stock in Merck and

585 Medtronic.

586 REFERENCES

- 587
- 588 Aaltonen, J., Björnses, P., Perheentupa, J., Horelli-Kuitunen, N., Palotie, A., Peltonen, L., Lee,
589 Y., Francis, F., Henning, S., Thiel, C., Leharach, H., & Yaspo, M. (1997). An autoimmune
590 disease, APECED, caused by mutations in a novel gene featuring two PHD-type zinc-finger
591 domains. *Nature Genetics*, *17*(4), 399–403. <https://doi.org/10.1038/ng1297-399>
- 592
- 593 Ackermann, K., Bux, R., Rüb, U., Korf, H.-W., Kauert, G., & Stehle, J. H. (2006).
594 Characterization of Human Melatonin Synthesis Using Autoptic Pineal Tissue. *Endocrinology*,
595 *147*(7), 3235–3242. <https://doi.org/10.1210/en.2006-0043>
- 596
- 597 Adriaenssens, A. E., Biggs, E. K., Darwish, T., Tadross, J., Sukthankar, T., Girish, M., Poley-
598 Wolf, J., Lam, B. Y., Zvetkova, I., Pan, W., Chiarugi, D., Yeo, G., Blouet, C., Gribble, F. M., &
599 Reimann, F. (2019). Glucose-Dependent Insulinotropic Polypeptide Receptor-Expressing Cells
600 in the Hypothalamus Regulate Food Intake. *Cell Metabolism*.
601 <https://doi.org/10.1016/j.cmet.2019.07.013>
- 602
- 603 Ahonen, P., Myllärniemi, S., Sipilä, I., & Perheentupa, J. (1990). Clinical Variation of
604 Autoimmune Polyendocrinopathy–Candidiasis–Ectodermal Dystrophy (APECED) in a Series of
605 68 Patients. *The New England Journal of Medicine*, *322*(26), 1829–1836.
606 <https://doi.org/10.1056/nejm199006283222601>
- 607
- 608 Akoury, E., Zhang, L., Ao, A., & Slim, R. (2015). NLRP7 and KHDC3L, the two maternal-
609 effect proteins responsible for recurrent hydatidiform moles, co-localize to the oocyte
610 cytoskeleton. *Human Reproduction (Oxford, England)*, *30*(1), 159–169.
611 <https://doi.org/10.1093/humrep/deu291>
- 612
- 613 Alanentalo, T., Chatonnet, F., Karlen, M., Sulniute, R., Ericson, J., Andersson, E., & Ahlgren, U.
614 (2006). Cloning and analysis of Nkx6.3 during CNS and gastrointestinal development. *Gene
615 Expression Patterns*, *6*(2), 162–170. <https://doi.org/10.1016/j.modgep.2005.06.012>
- 616
- 617 Alimohammadi, M., Björklund, P., Hallgren, A., Pöntynen, N., Szinnai, G., Shikama, N., Keller,
618 M. P., Ekwall, O., Kinkel, S. A., Husebye, E. S., Gustafsson, J., Rorsman, F., Peltonen, L.,
619 Betterle, C., Perheentupa, J., Akerström, G., Westin, G., Scott, H. S., Holländer, G. A., &
620 Kämpe, O. (2008). Autoimmune polyendocrine syndrome type 1 and NALP5, a parathyroid
621 autoantigen. *The New England Journal of Medicine*, *358*(10), 1018–1028.
622 <https://doi.org/10.1056/nejmoa0706487>
- 623
- 624 Alimohammadi, M., Dubois, N., Sköldbberg, F., Hallgren, Å., Tardivel, I., Hedstrand, H., Haavik,
625 J., Husebye, E. S., Gustafsson, J., Rorsman, F., Meloni, A., Janson, C., Vialettes, B., Kajosaari,
626 M., Egner, W., Sargur, R., Pontén, F., Amoura, Z., Grimfeld, A., ... Carel, J.-C. (2009).
627 Pulmonary autoimmunity as a feature of autoimmune polyendocrine syndrome type 1 and
628 identification of KCNRG as a bronchial autoantigen. *Proceedings of the National Academy of
629 Sciences*, *106*(11), 4396–4401. <https://doi.org/10.1073/pnas.0809986106>
- 630
- 631 Anderson. (2002). Projection of an Immunological Self Shadow Within the Thymus by the Aire

- 632 Protein. *Science*, 298(5597), 1395–1401. <https://doi.org/10.1126/science.1075958>
633
- 634 Baekkeskov, S., Aanstoot, H., Christgau, S., Reetz, A., Limena, Cascalho, M., Folli, F., Richter-
635 Olesen, H., Camilli, D. P., & Camilli, P. (1990). Identification of the 64K autoantigen in insulin-
636 dependent diabetes as the GABA-synthesizing enzyme glutamic acid decarboxylase. *Nature*,
637 347(6289), 151–156. <https://doi.org/10.1038/347151a0>
638
- 639 Bebbere, D., Masala, L., Albertini, D., & Ledda, S. (2016). The subcortical maternal complex:
640 multiple functions for one biological structure? *Journal of Assisted Reproduction and Genetics*,
641 33(11), 1–8. <https://doi.org/10.1007/s10815-016-0788-z>
642
- 643 Berger, M., Scheel, D. W., Macias, H., Miyatsuka, T., Kim, H., Hoang, P., Ku, G. M., Honig, G.,
644 Liou, A., Tang, Y., Regard, J. B., Sharifnia, P., Yu, L., Wang, J., Coughlin, S. R., Conklin, B. R.,
645 Deneris, E. S., Tecott, L. H., & German, M. S. (2015). Gα_i/o-coupled receptor signaling restricts
646 pancreatic β-cell expansion. *Proceedings of the National Academy of Sciences*, 112(9), 2888–
647 2893. <https://doi.org/10.1073/pnas.1319378112>
648
- 649 Berson, S. A., Yalow, R. S., Bauman, A., Rothschild, M. A., & Newerly, K. (1956). INSULIN-
650 I131 METABOLISM IN HUMAN SUBJECTS: DEMONSTRATION OF INSULIN BINDING
651 GLOBULIN IN THE CIRCULATION OF INSULIN TREATED SUBJECTS 1. *Journal of*
652 *Clinical Investigation*, 35(2), 170–190. <https://doi.org/10.1172/jci103262>
653
- 654 Betterle, C., Pra, C., Mantero, F., & Zanchetta, R. (2002). Autoimmune Adrenal Insufficiency
655 and Autoimmune Polyendocrine Syndromes: Autoantibodies, Autoantigens, and Their
656 Applicability in Diagnosis and Disease Prediction. *Endocrine Reviews*, 23(3), 327–364.
657 <https://doi.org/10.1210/edrv.23.3.0466>
658
- 659 Björk, E., Velloso, L. A., Kämpe, O., & Karlsson, A. F. (1994). GAD Autoantibodies in IDDM,
660 Stiff-Man Syndrome, and Autoimmune Polyendocrine Syndrome Type I Recognize Different
661 Epitopes. *Diabetes*, 43(1), 161–165. <https://doi.org/10.2337/diab.43.1.161>
662
- 663 Brozzetti, A., Alimohammadi, M., Morelli, S., Minarelli, V., Hallgren, A., Giordano, R., Bellis,
664 A., Perniola, R., Kämpe, O., & Falorni, A. (2015). Autoantibody Response Against
665 NALP5/MATER in Primary Ovarian Insufficiency and in Autoimmune Addison's Disease. *The*
666 *Journal of Clinical Endocrinology & Metabolism*, 100(5), 1941–1948.
667 <https://doi.org/10.1210/jc.2014-3571>
668
- 669 Bruserud, Ø., Oftedal, B. E., Landegren, N., Erichsen, M. M., Bratland, E., Lima, K., Jørgensen,
670 A. P., Myhre, A. G., Svartberg, J., Fougner, K. J., Bakke, Åsne, Nedrebø, B. G., Mella, B.,
671 Breivik, L., Viken, M. K., Knappskog, P. M., Marthinussen, M. C., Løvås, K., Kämpe, O., ...
672 Husebye, E. S. (2016). A Longitudinal Follow-up of Autoimmune Polyendocrine Syndrome
673 Type 1. *The Journal of Clinical Endocrinology & Metabolism*, 101(8), 2975–2983.
674 <https://doi.org/10.1210/jc.2016-1821>
675
- 676 Cheng, M., & Anderson, M. S. (2018). Thymic tolerance as a key brake on autoimmunity.
677 *Nature Immunology*, 19(7), 659–664. <https://doi.org/10.1038/s41590-018-0128-9>

- 678
679 Choi, H., Kim, T.-H., Yun, C.-Y., Kim, J.-W., & Cho, E.-S. (2016). Testicular acid phosphatase
680 induces odontoblast differentiation and mineralization. *Cell and Tissue Research*, *364*(1), 95–
681 103. <https://doi.org/10.1007/s00441-015-2310-9>
682
- 683 Clemente, M., Obermayer-Straub, P., Meloni, A., Strassburg, C. P., Arangino, V., Tukey, R. H.,
684 Virgiliis, S., & Manns, M. P. (1997). Cytochrome P450 1A2 Is a Hepatic Autoantigen in
685 Autoimmune Polyglandular Syndrome Type 1. *The Journal of Clinical Endocrinology &*
686 *Metabolism*, *82*(5), 1353–1361. <https://doi.org/10.1210/jcem.82.5.3913>
687
- 688 Conteduca, G., Indiveri, F., Filaci, G., & Negrini, S. (2018). Beyond APECED: An update on the
689 role of the AutoImmune regulator gene (AIRE) in physiology and disease. *Autoimmunity*
690 *Reviews*, *17*(Immunity 44 2016), 1 17. <https://doi.org/10.1016/j.autrev.2017.10.017>
691
- 692 DeVoss, J., Shum, A., Johannes, K., Lu, W., Krawisz, A., Wang, P., Yang, T., LeClair, N.,
693 Austin, C., Strauss, E., & Anderson. (2008). Effector Mechanisms of the Autoimmune Syndrome
694 in the Murine Model of Autoimmune Polyglandular Syndrome Type 1. *The Journal of*
695 *Immunology*, *181*(6), 4072–4079. <https://doi.org/10.4049/jimmunol.181.6.4072>
696
- 697 Du, Y. T., Rayner, C. K., Jones, K. L., Talley, N. J., & Horowitz, M. (2018). Gastrointestinal
698 Symptoms in Diabetes: Prevalence, Assessment, Pathogenesis, and Management. *Diabetes Care*,
699 *41*(3), 627–637. <https://doi.org/10.2337/dc17-1536>
700
- 701 Ekwall, O., Hedstrand, H., Grimelius, L., Haavik, J., Perheentupa, J., Gustafsson, J., Husebye,
702 E., Kämpe, O., & Rorsman, F. (1998). Identification of tryptophan hydroxylase as an intestinal
703 autoantigen. *The Lancet*, *352*(9124), 279–283. [https://doi.org/10.1016/s0140-6736\(97\)11050-9](https://doi.org/10.1016/s0140-6736(97)11050-9)
704
- 705 Ferré, E. M., Break, T. J., Burbelo, P. D., Allgäuer, M., Kleiner, D. E., Jin, D., Xu, Z., Folio, L.
706 R., Mollura, D. J., Swamydas, M., Gu, W., Hunsberger, S., Lee, C.-C. R., Bondici, A., Hoffman,
707 K. W., Lim, J. K., Dobbs, K., Niemela, J. E., Fleisher, T. A., ... Lionakis, M. S. (2019).
708 Lymphocyte-driven regional immunopathology in pneumonitis caused by impaired central
709 immune tolerance. *Science Translational Medicine*, *11*(495), eaav5597.
710 <https://doi.org/10.1126/scitranslmed.aav5597>
711
- 712 Ferré, E. M., Rose, S. R., Rosenzweig, S. D., Burbelo, P. D., Romito, K. R., Niemela, J. E.,
713 Rosen, L. B., Break, T. J., Gu, W., Hunsberger, S., Browne, S. K., Hsu, A. P., Rampertaap, S.,
714 Swamydas, M., Collar, A. L., Kong, H. H., Lee, C.-C., Chascsa, D., Simcox, T., ... Lionakis, M.
715 S. (2016). Redefined clinical features and diagnostic criteria in autoimmune polyendocrinopathy-
716 candidiasis-ectodermal dystrophy. *JCI Insight*, *1*(13), 1343–1349.
717 <https://doi.org/10.1172/jci.insight.88782>
718
- 719 Fishman, D., Kisand, K., Hertel, C., Rothe, M., Remm, A., Pihlap, M., Adler, P., Vilo, J., Peet,
720 A., Meloni, A., Podkrajsek, K., Battelino, T., Bruserud, Ø., Wolff, A. S., Husebye, E. S., Kluger,
721 N., Krohn, K., Ranki, A., Peterson, H., ... Peterson, P. (2017). Autoantibody Repertoire in
722 APECED Patients Targets Two Distinct Subgroups of Proteins. *Frontiers in Immunology*, *8*, 681
723 15. <https://doi.org/10.3389/fimmu.2017.00976>

- 724
725 Gavanescu, I., Benoist, C., & Mathis, D. (2008). B cells are required for Aire-deficient mice to
726 develop multi-organ autoinflammation: A therapeutic approach for APECED patients.
727 *Proceedings of the National Academy of Sciences*, *105*(35), 13009–13014.
728 <https://doi.org/10.1073/pnas.0806874105>
729
- 730 Gehart, H., van Es, J. H., Hamer, K., Beumer, J., Kretzschmar, K., Dekkers, J. F., Rios, A., &
731 Clevers, H. (2019). Identification of Enteroendocrine Regulators by Real-Time Single-Cell
732 Differentiation Mapping. *Cell*, *176*(Dev. Dyn. 194 1992), 1158–1173.e16.
733 <https://doi.org/10.1016/j.cell.2018.12.029>
734
- 735 Goldspink, D. A., Reimann, F., & Gribble, F. M. (2018). Models and Tools for Studying
736 Enteroendocrine Cells. *Endocrinology*, *159*(12), 3874–3884. [https://doi.org/10.1210/en.2018-](https://doi.org/10.1210/en.2018-00672)
737 [00672](https://doi.org/10.1210/en.2018-00672)
738
- 739 Hedstrand, H., Ekwall, O., Olsson, M. J., Landgren, E., Kemp, H. E., Weetman, A. P.,
740 Perheentupa, J., Husebye, E., Gustafsson, J., Betterle, C., Kämpe, O., & Rorsman, F. (2001). The
741 Transcription Factors SOX9 and SOX10 Are Vitiligo Autoantigens in Autoimmune
742 Polyendocrine Syndrome Type I. *Journal of Biological Chemistry*, *276*(38), 35390–35395.
743 <https://doi.org/10.1074/jbc.m102391200>
744
- 745 Högenauer, C., Meyer, R. L., Netto, G. J., Bell, D., Little, K. H., Ferries, L., Ana, C. A., Porter,
746 J. L., & Fordtran, J. S. (2001). Malabsorption Due to Cholecystokinin Deficiency in a Patient
747 with Autoimmune Polyglandular Syndrome Type I. *The New England Journal of Medicine*,
748 *344*(4), 270–274. <https://doi.org/10.1056/nejm200101253440405>
749
- 750 Holland, A. M., Hale, M. A., Kagami, H., Hammer, R. E., & MacDonald, R. J. (2002).
751 Experimental control of pancreatic development and maintenance. *Proceedings of the National*
752 *Academy of Sciences*, *99*(19), 12236–12241. <https://doi.org/10.1073/pnas.192255099>
753
- 754 Huhtaniemi, I., Hovatta, O., Marca, A., Livera, G., Monniaux, D., Persani, L., Heddar, A.,
755 Jarzabek, K., Laisk-Podar, T., Salumets, A., Tapanainen, J. S., Veitia, R. A., Visser, J. A.,
756 Wieacker, P., Wolczynski, S., & Misrahi, M. (2018). Advances in the Molecular
757 Pathophysiology, Genetics, and Treatment of Primary Ovarian Insufficiency. *Trends in*
758 *Endocrinology & Metabolism*, *29*(6), 400–419. <https://doi.org/10.1016/j.tem.2018.03.010>
759
- 760 Husebye, E. S., Anderson, M. S., & Kämpe, O. (2018). Autoimmune Polyendocrine Syndromes.
761 *The New England Journal of Medicine*, *378*(12), 1132–1141.
762 <https://doi.org/10.1056/nejmra1713301>
763
- 764 Husebye, E. S., Gebre-Medhin, G., Tuomi, T., Perheentupa, J., Landin-Olsson, M., Gustafsson,
765 J., Rorsman, F., & Kämpe, O. (1997). Autoantibodies against Aromatic L-Amino Acid
766 Decarboxylase in Autoimmune Polyendocrine Syndrome Type I. *The Journal of Clinical*
767 *Endocrinology & Metabolism*, *82*(1), 147–150. <https://doi.org/10.1210/jcem.82.1.3647>
768
- 769 Jasti, S., Warren, B. D., McGinnis, L. K., Kinsey, W. H., Petroff, B. K., & Petroff, M. G. (2012).

- 770 The Autoimmune Regulator Prevents Premature Reproductive Senescence in Female Mice1.
771 *Biology of Reproduction*, 86(4), 163–9. <https://doi.org/10.1095/biolreprod.111.097501>
772
- 773 Jeong, J., Jiang, L., Albino, E., Marrero, J., Rho, H., Hu, J., Hu, S., Vera, C., Bayron-
774 Poueymiroy, D., Rivera-Pacheco, Z., Ramos, L., Torres-Castro, C., Qian, J., Bonaventura, J.,
775 Boeke, J. D., Yap, W. Y., Pino, I., Eichinger, D. J., Zhu, H., & Blackshaw, S. (2012). Rapid
776 Identification of Monospecific Monoclonal Antibodies Using a Human Proteome Microarray.
777 *Molecular & Cellular Proteomics*, 11(6), O111.016253.
778 <https://doi.org/10.1074/mcp.o111.016253>
779
- 780 Kluger, N., Jokinen, M., Lintulahti, A., Krohn, K., & Ranki, A. (2015). Gastrointestinal
781 immunity against tryptophan hydroxylase-1, aromatic L-amino-acid decarboxylase, AIE-75,
782 villin and Paneth cells in APECED. *Clinical Immunology*, 158(2), 212–220.
783 <https://doi.org/10.1016/j.clim.2015.03.012>
784
- 785 Kuroda, N., Mitani, T., Takeda, N., Ishimaru, N., Arakaki, R., Hayashi, Y., Bando, Y., Izumi, K.,
786 Takahashi, T., Nomura, T., Sakaguchi, S., Ueno, T., Takahama, Y., Uchida, D., Sun, S., Kajiura,
787 F., Mouri, Y., Han, H., Matsushima, A., ... Matsumoto, M. (2005). Development of
788 Autoimmunity against Transcriptionally Unrepressed Target Antigen in the Thymus of Aire-
789 Deficient Mice. *The Journal of Immunology*, 174(4), 1862–1870.
790 <https://doi.org/10.4049/jimmunol.174.4.1862>
791
- 792 Landegren, N., Sharon, D., Freyhult, E., Hallgren, A., Eriksson, D., Edqvist, P.-H., Bensing, S.,
793 Wahlberg, J., Nelson, L. M., Gustafsson, J., Husebye, E. S., Anderson, M. S., Snyder, M., &
794 Kämpe, O. (2016). Proteome-wide survey of the autoimmune target repertoire in autoimmune
795 polyendocrine syndrome type 1. *Nature Publishing Group*, 6(1), 1–11.
796 <https://doi.org/10.1038/srep20104>
797
- 798 Landegren, N., Sharon, D., Shum, A. K., Khan, I. S., Fasano, K. J., Hallgren, Å., Kampf, C.,
799 Freyhult, E., Ardesjö-Lundgren, B., Alimohammadi, M., Rathsmann, S., Ludvigsson, J. F., Lundh,
800 D., Motrich, R., Rivero, V., Fong, L., Giwerzman, A., Gustafsson, J., Perheentupa, J., ... Kämpe,
801 O. (2015). Transglutaminase 4 as a prostate autoantigen in male subfertility. *Science*
802 *Translational Medicine*, 7(292), 292ra101–292ra101.
803 <https://doi.org/10.1126/scitranslmed.aaa9186>
804
- 805 Lanzavecchia, A. (1985). Antigen-specific interaction between T and B cells. *Nature*, 314(6011),
806 537–539. <https://doi.org/10.1038/314537a0>
807
- 808 Larman, B. H., Zhao, Z., Laserson, U., Li, M. Z., Ciccia, A., Gakidis, A. M., Church, G. M.,
809 Kesari, S., LeProust, E. M., Solimini, N. L., & Elledge, S. J. (2011). Autoantigen discovery with
810 a synthetic human peptidome. *Nature Biotechnology*, 29(6), 535–541.
811 <https://doi.org/10.1038/nbt.1856>
812
- 813 Leonard, J. D., Gilmore, D. C., Dileepan, T., Nawrocka, W. I., Chao, J. L., Schoenbach, M. H.,
814 Jenkins, M. K., Adams, E. J., & Savage, P. A. (2017). Identification of Natural Regulatory T Cell
815 Epitopes Reveals Convergence on a Dominant Autoantigen. *Immunity*, 47(1), 107–117.e8.

- 816 <https://doi.org/10.1016/j.immuni.2017.06.015>
817
- 818 Li, L., Baibakov, B., & Dean, J. (2008). A Subcortical Maternal Complex Essential for
819 Preimplantation Mouse Embryogenesis. *Developmental Cell*, *15*(3), 416–425.
820 <https://doi.org/10.1016/j.devcel.2008.07.010>
821
- 822 Liu, C., Li, M., Li, T., Zhao, H., Huang, J., Wang, Y., Gao, Q., Yu, Y., & Shi, Q. (2016). ECAT1
823 is essential for human oocyte maturation and pre-implantation development of the resulting
824 embryos. *Scientific Reports*, *6*(1), 38192. <https://doi.org/10.1038/srep38192>
825
- 826 Maclaren, N., Chen, Q., Kukreja, A., Marker, J., Zhang, C., & Sun, Z. (2001). Autoimmune
827 hypogonadism as part of an autoimmune polyglandular syndrome. *Journal of the Society for*
828 *Gynecologic Investigation*, *8*(1), S52–S54. [https://doi.org/10.1016/s1071-5576\(00\)00109-x](https://doi.org/10.1016/s1071-5576(00)00109-x)
829
- 830 Malchow, S., Leventhal, D. S., Lee, V., Nishi, S., Socci, N. D., & Savage, P. A. (2016). Aire
831 Enforces Immune Tolerance by Directing Autoreactive T Cells into the Regulatory T Cell
832 Lineage. *Immunity*, *44*(5), 1102–1113. <https://doi.org/10.1016/j.immuni.2016.02.009>
833
- 834 Mandel-Brehm, C., Dubey, D., Kryzer, T. J., O'Donovan, B. D., Tran, B., Vazquez, S. E.,
835 Sample, H. A., Zorn, K. C., Khan, L. M., Bledsoe, I. O., McKeon, A., Pleasure, S. J., Lennon, V.
836 A., DeRisi, J. L., Wilson, M. R., & Pittock, S. J. (2019). Kelch-like Protein 11 Antibodies in
837 Seminoma-Associated Paraneoplastic Encephalitis. *New England Journal of Medicine*, *381*(1),
838 47–54. <https://doi.org/10.1056/nejmoa1816721>
839
- 840 Meager, A., Visvalingam, K., Peterson, P., Möll, K., Murumägi, A., Krohn, K., Eskelin, P.,
841 Perheentupa, J., Husebye, E., Kadota, Y., & Willcox, N. (2006). Anti-Interferon Autoantibodies
842 in Autoimmune Polyendocrinopathy Syndrome Type 1. *PLoS Medicine*, *3*(7), e289.
843 <https://doi.org/10.1371/journal.pmed.0030289>
844
- 845 Meyer, S., Woodward, M., Hertel, C., Vlaicu, P., Haque, Y., Kärner, J., Macagno, A., Onuoha,
846 S. C., Fishman, D., Peterson, H., Metsküla, K., Uibo, R., Jääntti, K., Hokynar, K., Wolff, A. S.,
847 patient collaborative, A., Meloni, A., Kluger, N., Husebye, E. S., ... Hayday, A. (2016). AIRE-
848 Deficient Patients Harbor Unique High-Affinity Disease-Ameliorating Autoantibodies. *Cell*,
849 *166*(3), 582–595. <https://doi.org/10.1016/j.cell.2016.06.024>
850
- 851 Mitchell, J., Punthakee, Z., Lo, B., Bernard, C., Chong, K., Newman, C., Cartier, L., Desilets, V.,
852 Cutz, E., Hansen, I., Riley, P., & Polychronakos, C. (2004). Neonatal diabetes, with hypoplastic
853 pancreas, intestinal atresia and gall bladder hypoplasia: search for the aetiology of a new
854 autosomal recessive syndrome. *Diabetologia*, *47*(12), 2160–2167.
855 <https://doi.org/10.1007/s00125-004-1576-3>
856
- 857 Moody, A. J., Thim, L., & Valverde, I. (1984). The isolation and sequencing of human gastric
858 inhibitory peptide (GIP). *FEBS Letters*, *172*(2), 142–148. [https://doi.org/10.1016/0014-5793\(84\)81114-x](https://doi.org/10.1016/0014-5793(84)81114-x)
859
- 860
- 861 Nagamine, K., Peterson, P., Scott, H. S., Kudoh, J., Minoshima, S., Heino, M., Krohn, K. J.,

- 862 Lalioti, M. D., Mullis, P. E., Antonarakis, S. E., Kawasaki, K., Asakawa, S., Ito, F., & Shimizu,
863 N. (1997). Positional cloning of the APECED gene. *Nature Genetics*, *17*(4), 393–398.
864 <https://doi.org/10.1038/ng1297-393>
865
- 866 Nelson, L. M. (2009). Clinical practice. Primary ovarian insufficiency. *The New England*
867 *Journal of Medicine*, *360*(6), 606–614. <https://doi.org/10.1056/nejmcp0808697>
868
- 869 Obermayer-Straub, P., Strassburg, C., & Manns, M. (2000). Target Proteins in Human
870 Autoimmunity: Cytochromes P450 and Udp-Glycoronosyltransferases. *Canadian Journal of*
871 *Gastroenterology and Hepatology*, *14*(5), 429–439. <https://doi.org/10.1155/2000/910107>
872
- 873 O'Connor, D. T., Burton, D., & Deftos, L. J. (1983). Chromogranin A: Immunohistology reveals
874 its universal occurrence in normal polypeptide hormone producing endocrine glands. *Life*
875 *Sciences*, *33*(17), 1657–1663. [https://doi.org/10.1016/0024-3205\(83\)90721-x](https://doi.org/10.1016/0024-3205(83)90721-x)
876
- 877 O'Donovan, B., Mandel - Brehm, C., E. Vazquez, S., Liu, J., Paren, A. V., Anderson, M. S.,
878 Kassimatis, T., Zekeridou, A., Hauser, S. L., Pittock, S. J., Chow, E., Wilson, M. R., & DeRisi, J.
879 L. (2018). Exploration of Anti - Yo and Anti - Hu paraneoplastic neurological disorders
880 by PhIP - Seq reveals a highly restricted pattern of antibody epitopes. *Biorxiv.Org*.
881 <https://doi.org/10.1101/502187>
882
- 883 Oftedal, B. E., Hellesén, A., Erichsen, M. M., Bratland, E., Vardi, A., Perheentupa, J., Kemp, H.
884 E., Fiskerstrand, T., Viken, M. K., Weetman, A. P., Fleishman, S. J., Banka, S., Newman, W. G.,
885 Sewell, W. A. C., Sozaeva, L. S., Zayats, T., Haugarvoll, K., Orlova, E. M., Haavik, J., ...
886 Husebye, E. S. (2015). Dominant Mutations in the Autoimmune Regulator AIRE Are Associated
887 with Common Organ-Specific Autoimmune Diseases. *Immunity*, *42*(6), 1185–1196.
888 <https://doi.org/10.1016/j.immuni.2015.04.021>
889
- 890 Ohsie, S., Gerney, G., Gui, D., Kahana, D., Martín, M. G., & Cortina, G. (2009). A paucity of
891 colonic enteroendocrine and/or enterochromaffin cells characterizes a subset of patients with
892 chronic unexplained diarrhea/malabsorption. *Human Pathology*, *40*(7), 1006–1014.
893 <https://doi.org/10.1016/j.humpath.2008.12.016>
894
- 895 Oliva-Hemker, M., Berkenblit, G., Anhalt, G., & Yardley, J. (2006). Pernicious Anemia and
896 Widespread Absence of Gastrointestinal Endocrine Cells in a Patient with Autoimmune
897 Polyglandular Syndrome Type I and Malabsorption. *The Journal of Clinical Endocrinology &*
898 *Metabolism*, *91*(8), 2833–2838. <https://doi.org/10.1210/jc.2005-2506>
899
- 900 Otsuka, N., Tong, Z.-B., Vanevski, K., Tu, W., Cheng, M. H., & Nelson, L. M. (2011).
901 Autoimmune Oophoritis with Multiple Molecular Targets Mitigated by Transgenic Expression of
902 Mater. *Endocrinology*, *152*(6), 2465–2473. <https://doi.org/10.1210/en.2011-0022>
903
- 904 Patel, K. A., Kettunen, J., Laakso, M., Stančáková, A., Laver, T. W., Colclough, K., Johnson, M.
905 B., Abramowicz, M., Groop, L., Miettinen, P. J., Shepherd, M. H., Flanagan, S. E., Ellard, S.,
906 Inagaki, N., Hattersley, A. T., Tuomi, T., Cnop, M., & Weedon, M. N. (2017). Heterozygous
907 RFX6 protein truncating variants are associated with MODY with reduced penetrance. *Nature*

- 908 *Communications*, 8(1), 1–8. <https://doi.org/10.1038/s41467-017-00895-9>
909
- 910 Pederson, R. A., & McIntosh, C. H. (2016). Discovery of gastric inhibitory polypeptide and its
911 subsequent fate: Personal reflections. *Journal of Diabetes Investigation*, 7(S1), 4–7.
912 <https://doi.org/10.1111/jdi.12480>
913
- 914 Piccand, J., Vagne, C., Blot, F., Meunier, A., Beucher, A., Strasser, P., Lund, M. L., Ghimire, S.,
915 Nivlet, L., Lapp, C., Petersen, N., Engelstoft, M. S., Thibault-Carpentier, C., Keime, C., Correa,
916 S., Schreiber, V., Molina, N., Schwartz, T. W., Arcangelis, A., & Gradwohl, G. (2019). Rfx6
917 promotes the differentiation of peptide-secreting enteroendocrine cells while repressing genetic
918 programs controlling serotonin production. *Molecular Metabolism*, 29, 24–39.
919 <https://doi.org/10.1016/j.molmet.2019.08.007>
920
- 921 Pöntynen, N., Miettinen, A., Arstila, P. T., Kämpe, O., Alimohammadi, M., Vaarala, O.,
922 Peltonen, L., & Ulmanen, I. (2006). Aire deficient mice do not develop the same profile of
923 tissue-specific autoantibodies as APECED patients. *Journal of Autoimmunity*, 27(2), 96–104.
924 <https://doi.org/10.1016/j.jaut.2006.06.001>
925
- 926 Popler, J., Alimohammadi, M., Kämpe, O., Dalin, F., Dishop, M. K., Barker, J. M., Moriarty-
927 Kelsey, M., Soep, J. B., & Deterding, R. R. (2012). Autoimmune polyendocrine syndrome type
928 1: Utility of KCNRG autoantibodies as a marker of active pulmonary disease and successful
929 treatment with rituximab. *Pediatric Pulmonology*, 47(1), 84–87.
930 <https://doi.org/10.1002/ppul.21520>
931
- 932 Posovszky, C., Lahr, G., von Schnurbein, J., Buderus, S., Findeisen, A., Schröder, C., Schütz, C.,
933 Schulz, A., batin, K., Wabitsch, M., & Barth, T. (2012). Loss of Enteroendocrine Cells in
934 Autoimmune-Polyendocrine-Candidiasis-Ectodermal-Dystrophy (APECED) Syndrome with
935 Gastrointestinal Dysfunction. *The Journal of Clinical Endocrinology & Metabolism*, 97(2), E292
936 E300. <https://doi.org/10.1210/jc.2011-2044>
937
- 938 Puel, A., Döffinger, R., Natividad, A., Chrabieh, M., Barcenas-Morales, G., Picard, C., Cobat,
939 A., Ouachée-Chardin, M., Toulon, A., Bustamante, J., Al-Muhsen, S., Al-Owain, M., Arkwright,
940 P. D., Costigan, C., McConnell, V., Cant, A. J., Abinun, M., Polak, M., Bougnères, P.-F., ...
941 Casanova, J.-L. (2010). Autoantibodies against IL-17A, IL-17F, and IL-22 in patients with
942 chronic mucocutaneous candidiasis and autoimmune polyendocrine syndrome type I. *The*
943 *Journal of Experimental Medicine*, 207(2), 291–297. <https://doi.org/10.1084/jem.20091983>
944
- 945 Rath, M. F., Coon, S. L., Amaral, F. G., Weller, J. L., Møller, M., & Klein, D. C. (2016).
946 Melatonin Synthesis: Acetylserotonin O-Methyltransferase (ASMT) Is Strongly Expressed in a
947 Subpopulation of Pinealocytes in the Male Rat Pineal Gland. *Endocrinology*, 157(5), 2028–2040.
948 <https://doi.org/10.1210/en.2015-1888>
949
- 950 Reddy, R., Akoury, E., Nguyen, N., Abdul-Rahman, O. A., Dery, C., Gupta, N., Daley, W. P.,
951 Ao, A., Landolsi, H., Fisher, R., Touitou, I., & Slim, R. (2012). Report of four new patients with
952 protein-truncating mutations in C6orf221/KHDC3L and colocalization with NLRP7. *European*
953 *Journal of Human Genetics*, 21(9), 957–964. <https://doi.org/10.1038/ejhg.2012.274>

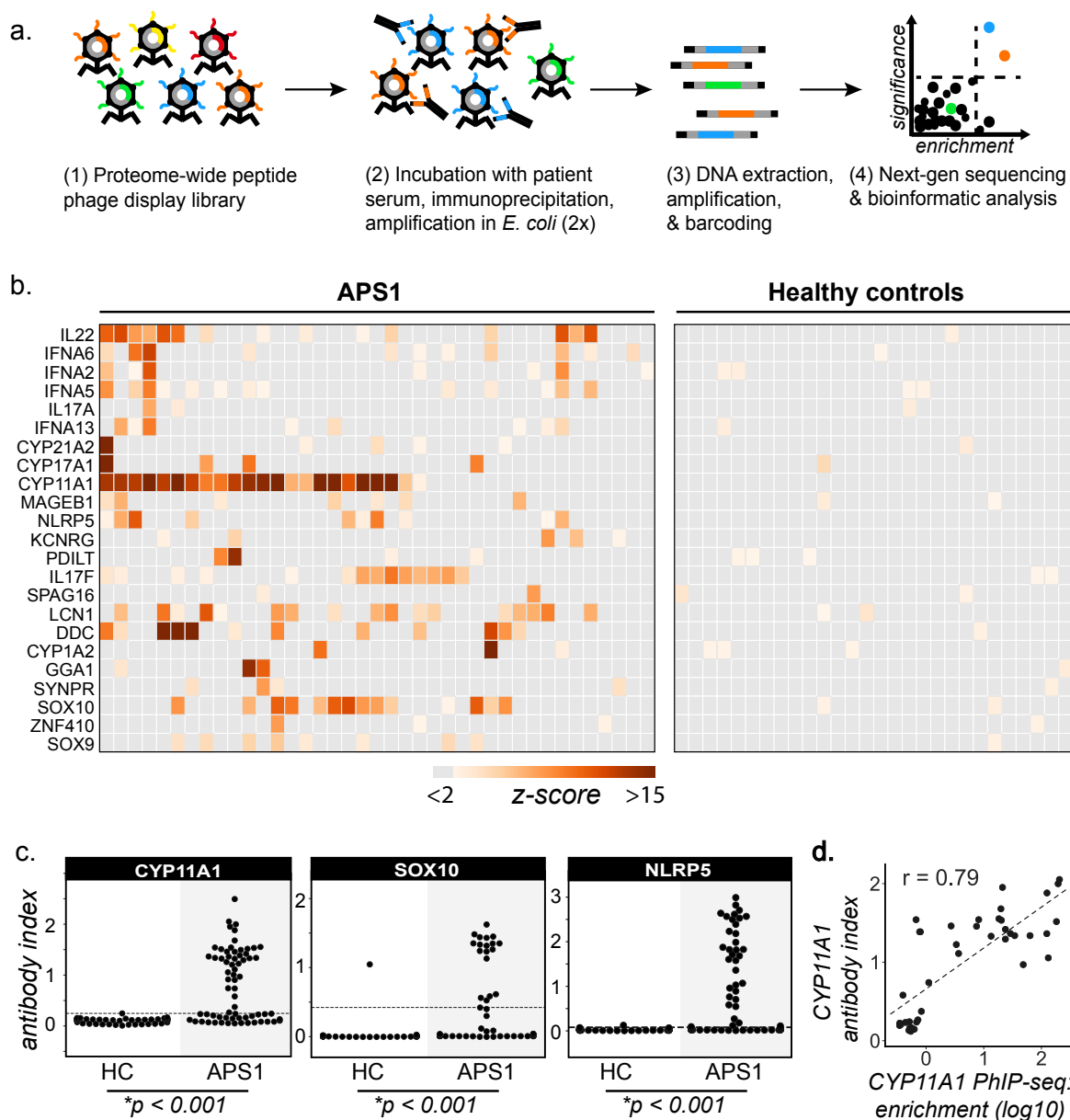
- 954
955 Rezaei, M., Nguyen, N., Foroughinia, L., Dash, P., Ahmadpour, F., Verma, I., Slim, R., &
956 Fardaei, M. (2016). Two novel mutations in the KHDC3L gene in Asian patients with recurrent
957 hydatidiform mole. *Human Genome Variation*, 3(1), 16027 5.
958 <https://doi.org/10.1038/hgv.2016.27>
959
- 960 Rosen, A., & Casciola-Rosen, L. (2014). Autoantigens as Partners in Initiation and Propagation
961 of Autoimmune Rheumatic Diseases. *Annual Review of Immunology*, 34(1), 1–26.
962 <https://doi.org/10.1146/annurev-immunol-032414-112205>
963
- 964 Sansom, S. N., Shikama-Dorn, N., Zhanybekova, S., Nusspaumer, G., Macaulay, I. C.,
965 Deadman, M. E., Heger, A., Ponting, C. P., & Holländer, G. A. (2014). Population and single-
966 cell genomics reveal the Aire dependency, relief from Polycomb silencing, and distribution of
967 self-antigen expression in thymic epithelia. *Genome Research*, 24(12), 1918–1931.
968 <https://doi.org/10.1101/gr.171645.113>
969
- 970 Schaum, N., Karkanias, J., Neff, N. F., May, A. P., Quake, S. R., Wyss-Coray, T., Darmanis, S.,
971 Batson, J., Botvinnik, O., Chen, M. B., Chen, S., Green, F., Jones, R. C., Maynard, A., Penland,
972 L., Pisco, A., Sit, R. V., anley, G., Webber, J. T., ... Wyss-Coray, T. (2018). Single-cell
973 transcriptomics of 20 mouse organs creates a Tabula Muris. *Nature*, 562(7727), 1 25.
974 <https://doi.org/10.1038/s41586-018-0590-4>
975
- 976 Seymen, F., Kim, Y., Lee, Y., Kang, J., Kim, T.-H., Choi, H., Koruyucu, M., Kasimoglu, Y.,
977 Tuna, E., Gencay, K., Shin, T., Hyun, H.-K., Kim, Y.-J., Lee, S.-H., Lee, Z., Zhang, H., Hu, J.,
978 Simmer, J. P., Cho, E.-S., & Kim, J.-W. (2016). Recessive Mutations in ACPT, Encoding
979 Testicular Acid Phosphatase, Cause Hypoplastic Amelogenesis Imperfecta. *The American*
980 *Journal of Human Genetics*, 99(5), 1199–1205. <https://doi.org/10.1016/j.ajhg.2016.09.018>
981
- 982 Sharon, D., & Snyder, M. (2014). Serum Profiling Using Protein Microarrays to Identify Disease
983 Related Antigens. *Methods in Molecular Biology (Clifton, N.J.)*, 1176, 169–178.
984 https://doi.org/10.1007/978-1-4939-0992-6_14
985
- 986 Shum, A. K., Alimohammadi, M., Tan, C. L., Cheng, M. H., Metzger, T. C., Law, C. S., Lwin,
987 W., Perheentupa, J., Bour-Jordan, H., Carel, J., Husebye, E. S., Luca, F., Janson, C., Sargur, R.,
988 Dubois, N., Kajosaari, M., Wolters, P. J., Chapman, H. A., Kämpe, O., & Anderson, M. S.
989 (2013). BPIFB1 is a lung-specific autoantigen associated with interstitial lung disease. *Science*
990 *Translational Medicine*, 5(206), 206ra139 206ra139.
991 <https://doi.org/10.1126/scitranslmed.3006998>
992
- 993 Shum, A. K., DeVoss, J., Tan, C. L., Hou, Y., Johannes, K., O’Gorman, C. S., Jones, K. D.,
994 Sochett, E. B., Fong, L., & Anderson, M. S. (2009). Identification of an autoantigen
995 demonstrates a link between interstitial lung disease and a defect in central tolerance. *Science*
996 *Translational Medicine*, 1(9), 9ra20 9ra20. <https://doi.org/10.1126/scitranslmed.3000284>
997
- 998 Sifuentes-Dominguez, L. F., Li, H., Llano, E., Liu, Z., Singla, A., Patel, A. S., Kathania, M.,
999 Khoury, A., Norris, N., Rios, J. J., Starokadomskyy, P., Park, J. Y., Gopal, P., Liu, Q., Tan, S.,

- 1000 Chan, L., Ross, T., Harrison, S., Venuprasad, K., ... Burstein, E. (2019). SCGN deficiency
1001 results in colitis susceptibility. *ELife*, 8, e49910. <https://doi.org/10.7554/elife.49910>
1002
- 1003 Silva, C., Yamakami, L., Aikawa, N., aujo, D., Carvalho, J., & Bonfá, E. (2014). Autoimmune
1004 primary ovarian insufficiency. *Autoimmunity Reviews*, 13(4–5), 427–430.
1005 <https://doi.org/10.1016/j.autrev.2014.01.003>
1006
- 1007 Smith, C. E., Whitehouse, L. L., Poulter, J. A., Brookes, S. J., Day, P. F., Soldani, F., Kirkham,
1008 J., Inglehearn, C. F., & Mighell, A. J. (2017). Defects in the acid phosphatase ACPT cause
1009 recessive hypoplastic amelogenesis imperfecta. *European Journal of Human Genetics*, 25(8),
1010 1015. <https://doi.org/10.1038/ejhg.2017.79>
1011
- 1012 Smith, S. B., Qu, H.-Q., Taleb, N., Kishimoto, N. Y., Scheel, D. W., Lu, Y., Patch, A.-M., Grabs,
1013 R., Wang, J., Lynn, F. C., Miyatsuka, T., Mitchell, J., Seerke, R., Désir, J., Eijnden, S.,
1014 Abramowicz, M., Kacet, N., Weill, J., Renard, M.-È., ... German, M. S. (2010). Rfx6 directs
1015 islet formation and insulin production in mice and humans. *Nature*, 463(7282), 775–780.
1016 <https://doi.org/10.1038/nature08748>
1017
- 1018 Sng, J., Ayoglu, B., Chen, J. W., Schickel, J.-N., Ferré, E. M., Glauzy, S., Romberg, N., Hoenig,
1019 M., Cunningham-Rundles, C., Utz, P. J., Lionakis, M. S., & Meffre, E. (2019). AIRE expression
1020 controls the peripheral selection of autoreactive B cells. *Science Immunology*, 4(34), eaav6778.
1021 <https://doi.org/10.1126/sciimmunol.aav6778>
1022
- 1023 Söderbergh, A., Myhre, A., Ekwall, O., Gebre-Medhin, G., Hedstrand, H., Landgren, E.,
1024 Miettinen, A., Eskelin, P., Halonen, M., Tuomi, T., Gustafsson, J., Husebye, E. S., Perheentupa,
1025 J., Gylling, M., Manns, M. P., Rorsman, F., Kämpe, O., & Nilsson, T. (2004). Prevalence and
1026 Clinical Associations of 10 Defined Autoantibodies in Autoimmune Polyendocrine Syndrome
1027 Type I. *The Journal of Clinical Endocrinology & Metabolism*, 89(2), 557–562.
1028 <https://doi.org/10.1210/jc.2003-030279>
1029
- 1030 Stoffers, D. A., Zinkin, N. T., Stanojevic, V., Clarke, W. L., & Habener, J. F. (1997). Pancreatic
1031 agenesis attributable to a single nucleotide deletion in the human IPF1 gene coding sequence.
1032 *Nature Genetics*, 15(1), 106–110. <https://doi.org/10.1038/ng0197-106>
1033
- 1034 Taplin, C. E., & Barker, J. M. (2009). Autoantibodies in type 1 diabetes. *Autoimmunity*, 41(1), 11
1035 18. <https://doi.org/10.1080/08916930701619169>
1036
- 1037 Uhlen, M., Fagerberg, L., Hallstrom, B., Lindskog, C., Oksvold, P., Mardinoglu, A., Sivertsson,
1038 A., Kampf, C., Sjostedt, E., Asplund, A., Olsson, I., Edlund, K., Lundberg, E., Navani, S.,
1039 Szigartyo, C., Odeberg, J., Djureinovic, D., Takanen, J., Hober, S., ... Ponten, F. (2015). Tissue-
1040 based map of the human proteome. *Science*, 347(6220), 1260419–1260419.
1041 <https://doi.org/10.1126/science.1260419>
1042
- 1043 Virant-Klun, I., Leicht, S., Hughes, C., & Krijgsveld, J. (2016). Identification of Maturation-
1044 Specific Proteins by Single-Cell Proteomics of Human Oocytes. *Molecular & Cellular*
1045 *Proteomics : MCP*, 15(8), 2616–2627. <https://doi.org/10.1074/mcp.m115.056887>

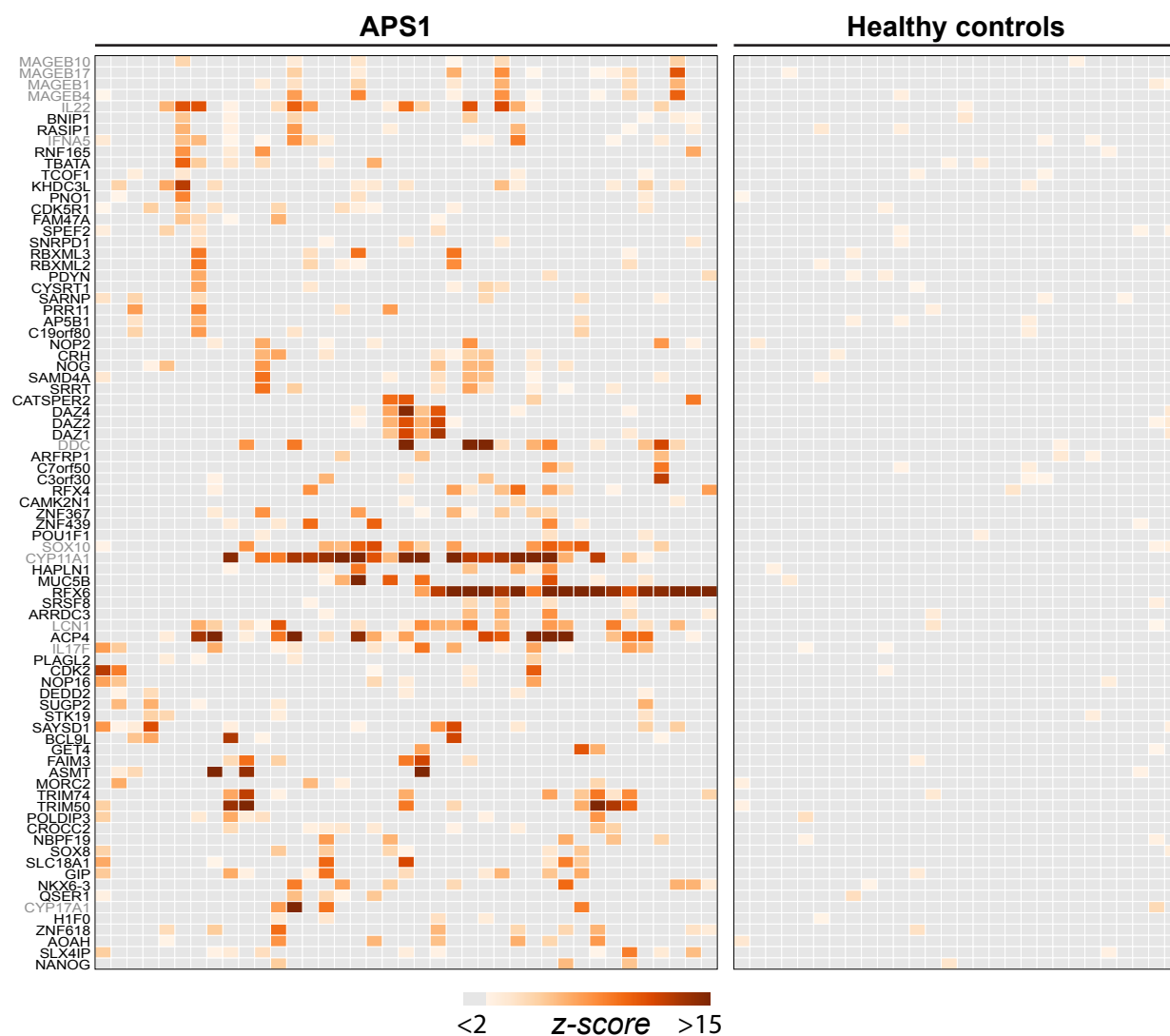
- 1046
1047 Wang, J., Cortina, G., Wu, V. S., Tran, R., Cho, J.-H., Tsai, M.-J., Bailey, T. J., Jamrich, M.,
1048 Ament, M. E., Treem, W. R., Hill, I. D., Vargas, J. H., Gershman, G., Farmer, D. G., Reyen, L.,
1049 & Martín, M. G. (2006). Mutant Neurogenin-3 in Congenital Malabsorptive Diarrhea. *The New*
1050 *England Journal of Medicine*, 355(3), 270–280. <https://doi.org/10.1056/nejmoa054288>
1051
1052 Wang, X., Song, D., Mykytenko, D., Kuang, Y., Lv, Q., Li, B., Chen, B., Mao, X., Xu, Y.,
1053 Zukin, V., Mazur, P., Mu, J., Yan, Z., Zhou, Z., Li, Q., Liu, S., Jin, L., He, L., Sang, Q., ...
1054 Wang, L. (2018). Novel mutations in genes encoding subcortical maternal complex proteins may
1055 cause human embryonic developmental arrest. *Reproductive BioMedicine Online*, 36(6), 698–
1056 704. <https://doi.org/10.1016/j.rbmo.2018.03.009>
1057
1058 Welt, C. K. (2008). Autoimmune Oophoritis in the Adolescent. *Annals of the New York Academy*
1059 *of Sciences*, 1135(1), 118–122. <https://doi.org/10.1196/annals.1429.006>
1060
1061 Winqvist, O., Gustafsson, J., Rorsman, F., Karlsson, F., & Kämpe, O. (1993). Two different
1062 cytochrome P450 enzymes are the adrenal antigens in autoimmune polyendocrine syndrome type
1063 I and Addison's disease. *Journal of Clinical Investigation*, 92(5), 2377–2385.
1064 <https://doi.org/10.1172/jci116843>
1065
1066 Wolff, A., Sarkadi, A., Maródi, L., Kärner, J., Orlova, E., Oftedal, B., Kisand, K., Oláh, É.,
1067 Meloni, A., Myhre, A., Husebye, E., Motaghedi, R., Perheentupa, J., Peterson, P., Willcox, N., &
1068 Meager, A. (2013). Anti-Cytokine Autoantibodies Preceding Onset of Autoimmune
1069 Polyendocrine Syndrome Type I Features in Early Childhood. *Journal of Clinical Immunology*,
1070 33(8), 1341–1348. <https://doi.org/10.1007/s10875-013-9938-6>
1071
1072 Zhang, W., Chen, Z., Zhang, D., Zhao, B., Liu, L., Xie, Z., Yao, Y., & Zheng, P. (2019).
1073 KHDC3L mutation causes recurrent pregnancy loss by inducing genomic instability of human
1074 early embryonic cells. *PLOS Biology*, 17(10), e3000468.
1075 <https://doi.org/10.1371/journal.pbio.3000468>
1076
1077 Zhang, Y., Yan, Z., Qin, Q., Nisenblat, V., Chang, H.-M., Yu, Y., Wang, T., Lu, C., Yang, M.,
1078 Yang, S., Yao, Y., Zhu, X., Xia, X., Dang, Y., Ren, Y., Yuan, P., Li, R., Liu, P., Guo, H., ...
1079 Yan, L. (2018). Transcriptome Landscape of Human Folliculogenesis Reveals Oocyte and
1080 Granulosa Cell Interactions. *Molecular Cell*, 72(6), 1–19.
1081 <https://doi.org/10.1016/j.molcel.2018.10.029>
1082
1083 Zhu, H., Bilgin, M., Bangham, R., Hall, D., Casamayor, A., Bertone, P., Lan, N., Jansen, R.,
1084 Bidlingmaier, S., Houfek, T., Mitchell, T., Miller, P., Dean, R. A., Gerstein, M., & Snyder, M.
1085 (2001). Global Analysis of Protein Activities Using Proteome Chips. *Science*, 293(5537), 2101–
1086 2105. <https://doi.org/10.1126/science.1062191>
1087
1088 Zhu, K., Yan, L., Zhang, X., Lu, X., Wang, T., Yan, J., Liu, X., Qiao, J., & Li, L. (2015).
1089 Identification of a human subcortical maternal complex. *Molecular Human Reproduction*, 21(4),
1090 320–329. <https://doi.org/10.1093/molehr/gau116>
1091

1092 Ziegler, B., Schlosser, M., Lühder, F., Strebelow, M., Augstein, P., Northemann, W., Powers, A.,
1093 & Ziegler, M. (1996). Murine monoclonal glutamic acid decarboxylase (GAD)65 antibodies
1094 recognize autoimmune-associated GAD epitope regions targeted in patients with type 1 diabetes
1095 mellitus and Stiff-man syndrome. *Acta Diabetologica*, 33(3), 225–231.
1096 <https://doi.org/10.1007/bf02048548>
1097

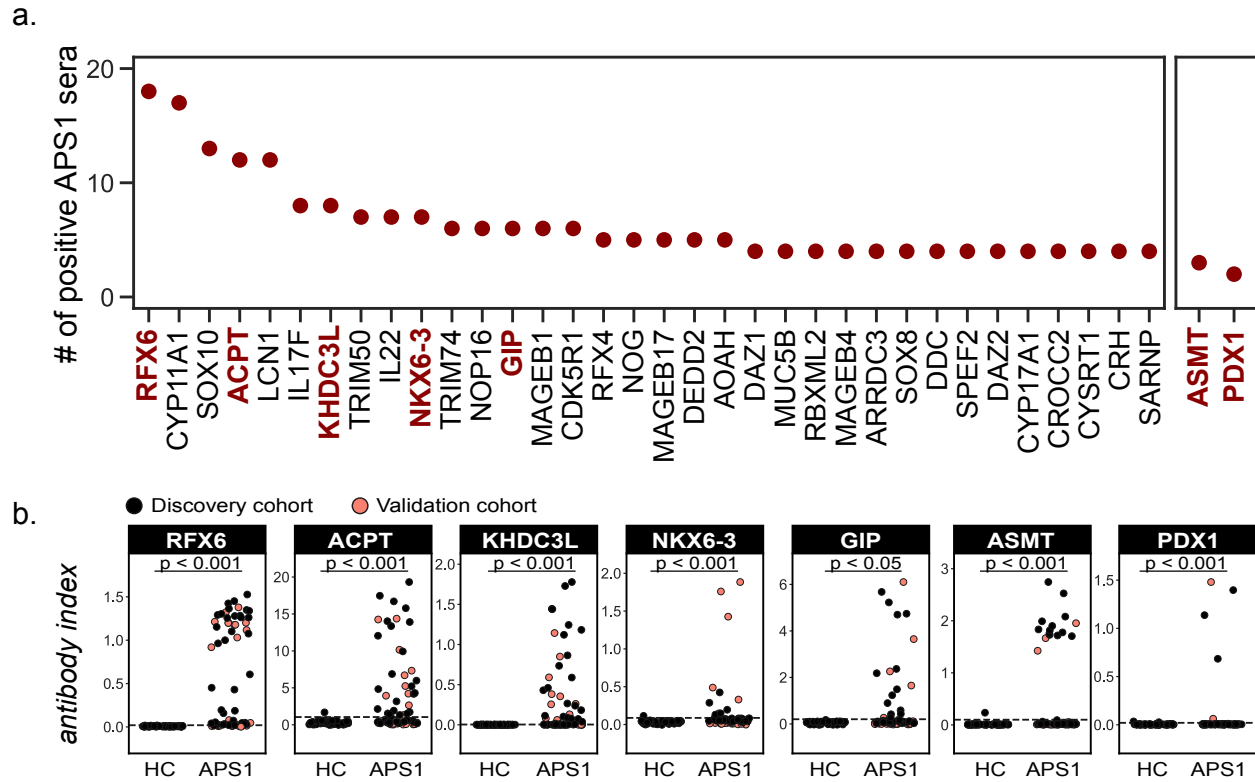
1098 FIGURES



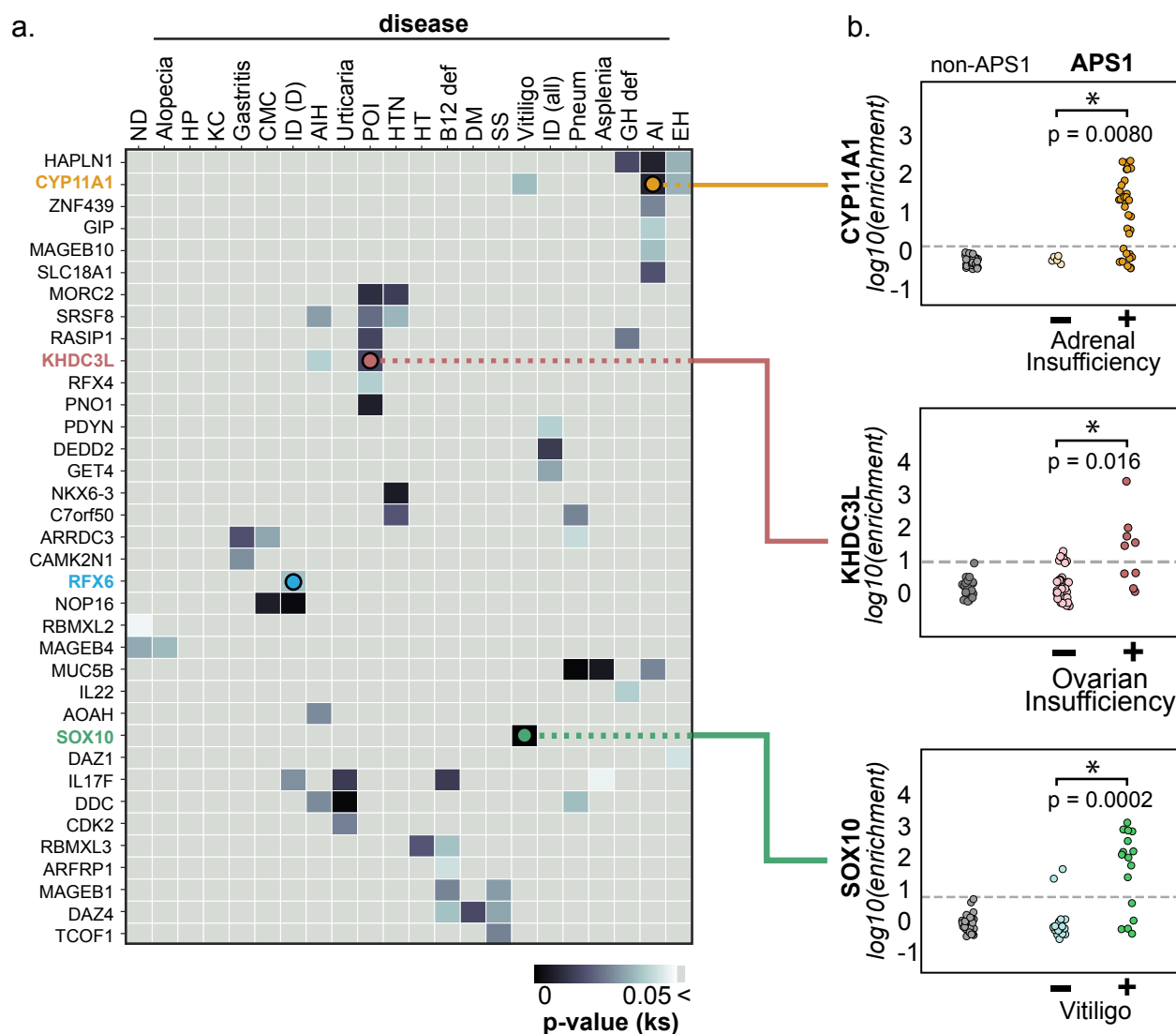
1099
1100 **Figure 1. PhIP-Seq identifies literature-reported autoantigens in APS1** **A.** Overview of PhIP-
1101 Seq experimental workflow. **B.** PhIP-Seq identifies known autoantibody targets in APS1.
1102 Hierarchically clustered (Pearson) z-scored heatmap of literature reported autoantigens with 10-
1103 fold or greater signal over mock-IP in at least 2/39 APS1 sera and in 0/28 non-APS1 control sera.
1104 See also [Figure 1: Figure Supplement 1](#). **C.** Radioligand binding assay (RLBA) orthogonal
1105 validation of literature-reported antigens CYP11A1, SOX10, and NLRP5 within the expanded
1106 cohort of APS1 ($n = 67$) and non-APS1 controls ($n = 61$); p-value was calculated across all samples
1107 using a Mann-Whitney U test. **D.** CYP11A1 RLBA antibody index and CYP11A1 PhIP-Seq
1108 enrichment are well correlated ($r = 0.79$); see also [Figure 1: Figure Supplement 2](#).



1109 **Figure 2. PhIP-Seq identifies novel (and known) antigens across multiple APS1 sera. A.**
1110 Hierarchically clustered (Pearson) Z-scored heatmap of all genes with 10-fold or greater signal
1111 over mock-IP in at least 3/39 APS1 sera and in 0/28 non-APS1 sera. Black labeled antigens (n=69)
1112 are potentially novel and grey labeled antigens (n=12) are previously literature-reported antigens.
1113 See also [Figure 2: Figure Supplement 1](#).



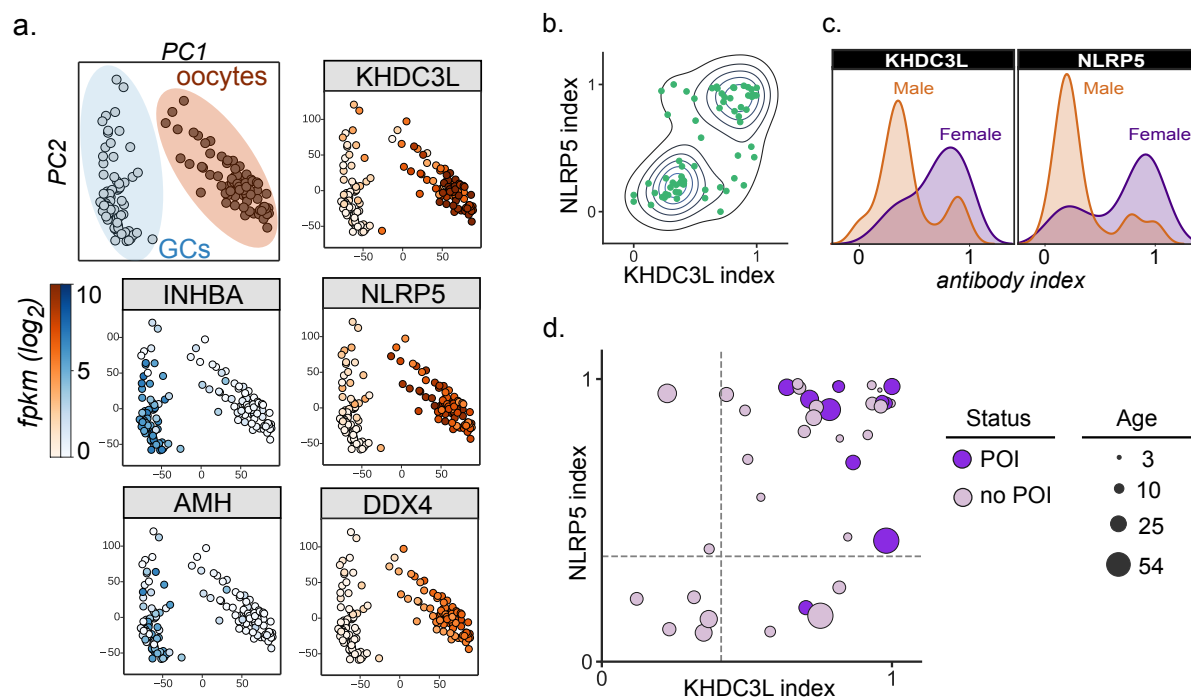
1114 **Figure 3. Novel PhIP-Seq autoantigens are shared across multiple APS1 samples and**
1115 **validate in whole protein binding assays. A.** Graph of the PhIP-seq autoantigens from Figure 2
1116 that were shared across the highest number of individual APS1 sera (left panel). ASMT and PDX1
1117 were positive hits in 3 and 2 sera, respectively, but are known to be highly tissue specific (right
1118 panel). Genes in red were chosen for validation in whole protein binding assay. **B.** Validation of
1119 novel PhIP-Seq antigens by radiolabeled binding assay, with discovery cohort (black, $n_{\text{APS1}} = 39$),
1120 validation cohort (light red, $n_{\text{APS1}} = 28$) and non-APS1 control cohort ($n_{\text{HC}} = 61$). P-value was
1121 calculated across all samples using a Mann-Whitney U test. See also [Figure 3: Figure Supplement](#)
1122 [1](#).



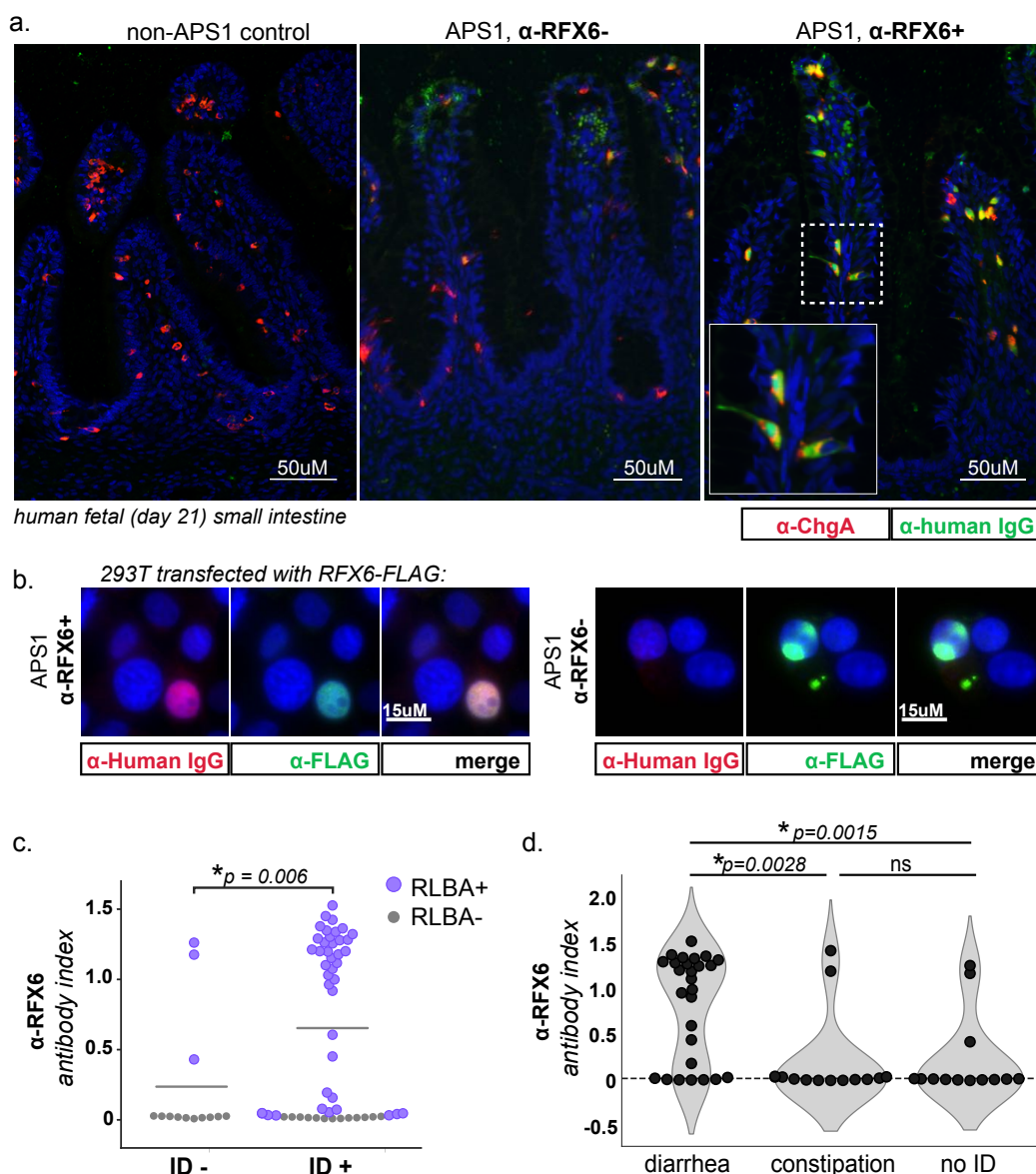
1123 **Figure 4. PhIP-Seq reproduces known clinical associations with anti-CYP11A1 and anti-**
 1124 **SOX10 antibodies.** **A.** Heatmap of p-values (Kolmogorov-Smirnov testing) for differences in
 1125 gene enrichments for individuals with versus without each clinical phenotype. Significant p-values
 1126 in the negative direction (where mean PhIP-Seq enrichment is higher in individuals without
 1127 disease) are masked (colored >0.05). See also [Figure 4: Figure Supplement 1](#). **B.** Anti-CYP11A1
 1128 PhIP-Seq enrichments are significantly different between APS1 patients with and without adrenal
 1129 insufficiency (top panel; Kolmogorov-Smirnov test). Anti-SOX10 PhIP-Seq enrichments are
 1130 significantly different between APS1 patients with and without Vitiligo (bottom panel). Anti-
 1131 KHDC3L PhIP-Seq enrichments are significantly different between APS1 patients with and
 1132 without ovarian insufficiency (middle panel). See also [Figure 4: Figure Supplement 2](#).

1133
 1134 ND, nail dystrophy. HP, hypoparathyroidism. KC, keratoconjunctivitis. CMC, chronic
 1135 mucocutaneous candidiasis. ID (D), Intestinal dysfunction (diarrheal-type). AIH, autoimmune
 1136 hepatitis. POI, primary ovarian insufficiency. HTN, hypertension. HT, hypothyroidism. B12 def,

1137 B12 (vitamin) deficiency. DM, diabetes mellitus. SS, Sjogren's-like syndrome. Pneum,
1138 Pneumonitis. GH def, Growth hormone deficiency. AI, Adrenal Insufficiency. EH, (dental) enamel
1139 hypoplasia.



1140
 1141 **Figure 5. Autoantibodies to oocyte-expressed protein KHDC3L are associated with ovarian**
 1142 **insufficiency. A.** Principle component analysis of transcriptome of single human oocytes (red)
 1143 and granulosa cells (GCs, blue); data from Zhang et al., Mol Cell 2018. KHDC3L is highly
 1144 expressed in oocytes, along with binding partner NLRP5 and known oocyte marker DDX4. For
 1145 comparison, known GC markers INHBA and AMH are primarily expressed in the GC population.
 1146 **B.** APS1 sera that are positive for one of anti-KHDC3L and anti-NLRP5 autoantibodies tend to
 1147 also be positive for the other. **C.** Antibody indices for both KHDC3L and NLRP5 are increased in
 1148 females with APS1. **D.** Antibody indices for females with APS1 by age; All 10 patients with
 1149 primary ovarian insufficiency (POI) are positive for anti-KHDC3L antibodies. Of note, many of
 1150 the individuals with anti-KHDC3L antibodies but without POI are younger and therefore cannot
 1151 be fully evaluated for ovarian insufficiency.



1152 **Figure 6. APS1 patients with intestinal dysfunction mount an antibody response to intestinal**
 1153 **enteroendocrine cells and to enteroendocrine-expressed protein RFX6. A.** Anti-RFX6 positive
 1154 APS1 serum with intestinal dysfunction co-stains Chromogranin-A (ChgA) positive
 1155 enteroendocrine cells in a nuclear pattern (right panel & inset). In contrast, non-APS1 control sera
 1156 as well as anti-RFX6 negative APS1 serum do not co-stain ChgA+ enteroendocrine cells (left and
 1157 center panels). **B.** Anti-RFX6+ serum, but not anti-RFX6- serum, co-stains HEK293T cells
 1158 transfected with an RFX6-expressing plasmid. See also [Figure 6: Figure Supplement 2](#). **C.**
 1159 Radioligand binding assay (RLBA) anti-RFX6 antibody index is significantly higher across
 1160 individuals with intestinal dysfunction (ID; Mann-Whitney U, $p = 0.006$). Purple color indicates
 1161 samples that fall above 6 standard deviations of the mean non-APS1 control RLBA antibody index.
 1162 **D.** Individuals with the diarrheal subtype of ID have a higher frequency of anti-RFX6 antibody
 1163 positivity as compared to those with constipation-type ID (Mann-Whitney U, $p = 0.0028$) or no ID
 1164 ($p = 0.0015$). See also [Figure 6: Figure Supplement 3](#).
 1165 For associated RFX6 PhIP-Seq & tissue expression data, see [Figure 6: Figure Supplement 1](#).

1166 SUPPLEMENTAL FIGURES

1167 Supplemental Table 1. APS1 cohort: Clinical Data.

| Patient Code | Gender | Age* | Clinical Phenotypes | Cohort |
|--------------|--------|------|---|----------|
| AIRE.04 | F | 14 | CMC, HP, AI, DM, EH, ND, HTN, SS, Pneumonitis, UE, GH def, ID (D) | D |
| AIRE.05 | F | 11 | CMC, HP, AI, AIH, Gastritis, EH, HTN, Pneumonitis, UE, Vitiligo, ID (B) | D |
| AIRE.09 | F | 10 | HP, AIH, EH, Pneumonitis, UE | D |
| AIRE.13 | F | 10 | CMC, HP, AI, Gastritis, UE, Vitiligo, ID (D) | D |
| AIRE.14 | M | 7 | CMC, AI, AIH, DM, Gastritis, EH, ND, KC, SS, Pneumonitis, UE, Vitiligo, B12 def, ID (C) | D |
| AIRE.18 | F | 18 | CMC, HP, AI, POI, ND, SS | D |
| AIRE.19 | M | 12 | CMC, HP, AI, AIH, Gastritis, EH, Pneumonitis, UE, GH def, Asplenia, ID (B) | D |
| AIRE.20 | F | 25 | CMC, AI, Gastritis, EH, KC, SS, ID (D) | D |
| AIRE.21 | M | 65 | CMC, HP, AI, HT, DM, EH, HTN, SS, Vitiligo, B12 def, ID (B) | D |
| AIRE.23 | M | 38 | CMC, HP, AI, Gastritis, TIN, EH, ND, KC, HTN, Vitiligo, Alopecia, B12 def, Asplenia, ID (D) | D |
| AIRE.24 | F | 15 | CMC, HP, AI, AIH, Gastritis, EH, KC, ID (C) | D |
| AIRE.27 | M | 18 | CMC, AI, AIH, DM, Gastritis, EH, KC, SS, Pneumonitis, UE, Vitiligo, B12 def, ID (B) | D |
| AIRE.08 | M | 11 | CMC, HP, AI, EH, UE | D |
| AIRE.07 | M | 12 | CMC, HP, AI, HT, ND, KC, Alopecia, ID (C) | D |
| AIRE.28 | M | 15 | CMC, HP, AI, Gastritis, EH, KC, Vitiligo, ID (C) | D |
| AIRE.22 | F | 7 | CMC, HP, AIH, Gastritis, EH, ND, SS, Pneumonitis, UE, Alopecia, GH def, ID (D) | D |
| AIRE.29 | M | 9 | AI, AIH, EH, ND, UE, Vitiligo, Alopecia, ID (B) | D |
| AIRE.30 | M | 17 | CMC, HP, AIH, EH, UE, Vitiligo, Alopecia, B12 def, ID (C) | D |
| AIRE.23c | F | 41 | CMC, HP, AI, HT, POI, EH, SS | D |
| AIRE.31 | F | 18 | CMC, HP, AI, AIH, DM, EH, ND, KC, SS, UE, Vitiligo, ID (D) | D |
| AIRE.33 | F | 14 | HP, AI, AIH, POI, EH, UE, ID (D) | D |
| AIRE.34 | F | 54 | CMC, HP, AI, HT, POI, Gastritis, EH, HTN, SS, Pneumonitis, B12 def, ID (D) | D |
| AIRE.35 | F | 23 | CMC, HP, AI, AIH, HT, POI, Gastritis, EH, SS, Pneumonitis, UE, B12 def, Asplenia, ID (D) | D |

| | | | | |
|---------|---|----|---|----------|
| AIRE.11 | M | 19 | CMC, HP, AI, AIH, TF, Gastritis, EH, SS, UE, Vitiligo, GH def, ID (B) | D |
| AIRE.36 | M | 15 | HP, AI, EH, Alopecia | D |
| AIRE.37 | F | 28 | CMC, HP, AI, POI, EH, SS, UE, ID (D) | D |
| AIRE.38 | F | 7 | HP, AI, EH, ND, UE, Alopecia, ID (C) | D |
| AIRE.17 | F | 6 | CMC, HP, EH, KC, UE, ID (D) | D |
| AIRE.39 | F | 18 | CMC, HP, AI, AIH, HT, EH, ND, KC, Pneumonitis, UE, ID (B) | D |
| AIRE.40 | F | 16 | CMC, HP, AI, AIH, POI, EH, Pneumonitis, UE, Alopecia, Asplenia, ID (D) | D |
| AIRE.41 | M | 20 | CMC, AI, HT, TF, EH, HTN, Vitiligo, Alopecia, ID (D) | D |
| AIRE.44 | F | 24 | CMC, HP, AI, POI, Gastritis, EH, ND, KC, HTN, SS, UE, Alopecia, B12 def, ID (D) | D |
| AIRE.46 | F | 22 | CMC, HP, AI, EH, KC, SS, B12 def, GH def, ID (B) | D |
| AIRE.12 | F | 7 | CMC, HP, AI, Gastritis, EH, KC, SS, Pneumonitis, UE, Vitiligo, B12 def, ID (D) | D |
| AIRE.06 | F | 16 | CMC, HP, AI, AIH, HT, Gastritis, EH, HTN, SS, Vitiligo, ID (D) | D |
| AIRE.50 | F | 26 | CMC, AI, Gastritis, HTN, SS, Pneumonitis, UE, B12 def, ID (B) | D |
| AIRE.02 | M | 51 | CMC, HP, AI, TF, Gastritis, EH, HTN, SS, Hpit, Pneumonitis, Vitiligo, B12 def, ID (D) | D |
| AIRE.03 | F | 19 | HP, AI, POI, TIN, EH, HTN, Pneumonitis, UE | D |
| AIRE.52 | F | 9 | HP, HT, EH, UE, Vitiligo, ID (D) | D |
| AIRE.53 | F | 8 | CMC, HP, AI, HT, EH, HTN, UE, ID (D) | V |
| AIRE.58 | M | 16 | CMC, HP, AI, TF, Gastritis, EH, ND, KC, Alopecia, B12 def, ID (D) | V |
| AIRE.59 | M | 7 | CMC, HP, AI, EH, ND, Alopecia, ID (D) | V |
| AIRE.60 | M | 19 | CMC, ND, EH, Alopecia, ID (C) | V |
| AIRE.61 | F | 54 | CMC, HP, AI, EH, SS, Pneumonitis, ID (C) | V |
| AIRE.62 | F | 15 | AI, AIH, HT, Gastritis, Pneumonitis, UE, ID (C) | V |
| AIRE.55 | M | 19 | CMC, HP, AI, Gastritis, EH, UE, Alopecia | V |
| AIRE.69 | M | 18 | CMC, AI, AIH, ID (B) | V |
| AIRE.56 | M | 2 | AIH, EH, UE, ID (D) | V |
| AIRE.54 | F | 7 | CMC, HP, AI, EH, Pneumonitis, UE | V |
| AIRE.63 | F | 15 | CMC, HP, AI, EH, B12 def, ID (B) | V |

| | | | | |
|----------|---|----|--|---|
| AIRE.71 | F | 30 | CMC, HP, Gastritis, EH, Pneumonitis, Vitiligo, ID (D) | V |
| AIRE.71B | M | 15 | CMC, AI, HT, Gastritis, ND, Pneumonitis, Alopecia | V |
| AIRE.74 | F | 11 | CMC, HP, AI, HT, Gastritis, TIN, EH, SS, Pneumonitis, UE, Alopecia, ID (C) | V |
| AIRE.68 | F | 15 | CMC, AI, Gastritis, EH, SS, Pneumonitis, B12 def, ID (C) | V |
| AIRE.70 | F | 16 | CMC, SS, UE, B12 def, ID (C) | V |
| AIRE.66 | M | 13 | CMC, HP, AI, DM, EH, UE, Alopecia | V |
| AIRE.67 | M | 20 | CMC, HP, AI, Pneumonitis, UE, Vitiligo, ID (D) | V |
| AIRE.87 | F | 15 | CMC, HP, AI, AIH, HT, EH, Pneumonitis, Vitiligo, B12 def, ID (B) | V |
| AIRE.65C | M | 2 | CMC, HP, AI, UE, ID (C) | V |
| AIRE.65B | M | 6 | CMC, HP, AI, EH | V |
| AIRE.65 | F | 11 | CMC, HP, AI, EH, UE, Vitiligo, GH def, ID (D) | V |
| AIRE.73 | F | 13 | CMC, HP, AIH, HT, POI, EH, ID (B) | V |
| AIRE.76 | M | 10 | CMC, HP, UE, Vitiligo, ID (D) | V |
| AIRE.86 | F | 3 | HP, UE, ID (C) | V |
| AIRE.77 | M | 10 | HP, AIH, HT, SS, Pneumonitis, Vitiligo, Alopecia, ID (D) | V |
| AIRE.78 | M | 2 | HP | V |
| AIRE.79 | M | 10 | CMC, HP, AI, AIH, EH, UE, GH def, Asplenia | V |

1168

1169 ND, nail dystrophy. HP, hypoparathyroidism. KC, keratoconjunctivitis. CMC, chronic
 1170 mucocutaneous candidiasis. ID (D, C, B), Intestinal dysfunction (diarrheal-type, constipation-type,
 1171 both). AIH, autoimmune hepatitis. POI, primary ovarian insufficiency. HTN, hypertension. HT,
 1172 hypothyroidism. B12 def, B12 (vitamin) deficiency. DM, diabetes mellitus. SS, Sjogren's-like
 1173 syndrome. GH def, Growth hormone deficiency. AI, Adrenal Insufficiency. EH, (dental) enamel
 1174 hypoplasia. TF, testicular failure. TIN, Tubulointerstitial Nephritis. Hpit, Hypopituitarism. UE,
 1175 Urticarial eruption.

1176 D, Discovery cohort; V, Validation cohort.

1177 *Age at most recent evaluation

1178

1179 **Supplemental Table 2. Tissue-restricted expression patterns of validated novel APS1**
 1180 **antigens.**

| Gene (Human/mouse) | Protein Atlas: RNA specificity category (Tissue)¹⁴ | Selected literature annotations |
|-------------------------------|--|---|
| <i>RFX6/Rfx6</i> | Tissue enhanced | Pancreas Islets (Piccand et al., 2014; S. B. Smith et al., 2010) Intestine Enteroendocrine cells (Gehart et al., 2019; Piccand et al., 2019; S. B. Smith et al., 2010) |
| <i>KHDC3L/Khdc3</i> | Group enriched | Ovary Oocytes (Y. Zhang et al., 2018; K. Zhu et al., 2015) |
| <i>ACP4/Acp4</i> | Tissue enhanced | Testes (Yousef et al., 2001) Dental enamel (Green et al., 2019; Seymen et al., 2016; C. E. Smith et al., 2017) |
| <i>ASMT/Asmt</i> | Tissue enhanced | Brain Pineal Gland (Rath et al., 2016) |
| <i>GIP/Gip</i> | Tissue enriched | Intestine Enteroendocrine cells (Moody et al., 1984) |
| <i>NKX6-3 / Nkx6-3</i> | Group enriched | Pancreas PP-cells (Schaum et al., 2018) Intestine (Alanentalo et al., 2006) |
| <i>PDX1 / Pdx1</i> | Group enriched | Pancreas Islets (Holland et al., 2002; Stoffers et al., 1997) |

1181

1182

1183 **Supplemental Table 3. Antibody information by application.**

| antibody | Application (IF: immunofluorescence; RLBA: radioligand binding assay; CBA: cell-based assay) | dilution |
|---|---|--|
| Anti-NLRP5 (Santa Cruz, Dallas, TX; #sc-50630) | NLRP5 RLBA | 1:50 |
| Anti-SOX10 (Abcam, Cambridge, MA, #ab181466) | SOX10 RLBA | 1:25 |
| Anti-RFX6 (R&D Systems, Minneapolis, MN; #AF7780) | RFX6 RLBA | 1:50 |
| Anti-KHDC3L (Abcam, #ab170298) | KHDC3L RLBA | 1:25 |
| Anti-CYP11A1 (Abcam, #ab175408) | CYP11A1 RLBA | 1:50 |
| Anti-NKX6-3 (Biorbyt, Cambridge, Cambridgeshire, UK; #orb127108) | NKX6-3 RLBA | 1:50 |
| Anti-GIP (Abcam, #ab30679) | GIP RLBA | 1:50 |
| Anti-PDX1 (Invitrogen, Carlsbad, CA, #PA5-78024) | PDX1 RLBA | 1:50 |
| Anti-ASMT (Invitrogen, #PA5-24721) | ASMT RLBA | 1:25 |
| Anti-CHGA (Abcam, Cambridge, MA, USA, #ab15160) | Tissue IF | 1:5000 |
| Human serum | Tissue IF CBA IF RLBA | 1:4000 (Tissue) 1:500 (CBA) 1:25 (RLBA) |
| Secondary abs: 488 goat anti-human IgG (Life Technologies, Waltham, MA, USA: #A11013) 546 goat anti-rabbit IgG (Life Technologies, A11010) | Tissue IF | 1:400 |
| Secondary abs: 647 goat anti-human IgG (Thermo Fisher, #A-21445) 488 goat anti-rabbit IgG (Thermo Fisher, #A-11034) | CBA IF | 1:1000 |
| Anti-DYKDDDDK (D6W5B) (Cell Signaling Technologies, Danvers, MA; #14793) | CBA IF; ACP4 RLBA | 1:2000 (CBA IF) 1:125 (RLBA) |
| Nuclear staining: Hoechst dye (Invitrogen, #33342) DAPI (Thermo Fisher, #D1306) | Tissue IF CBA IF | |

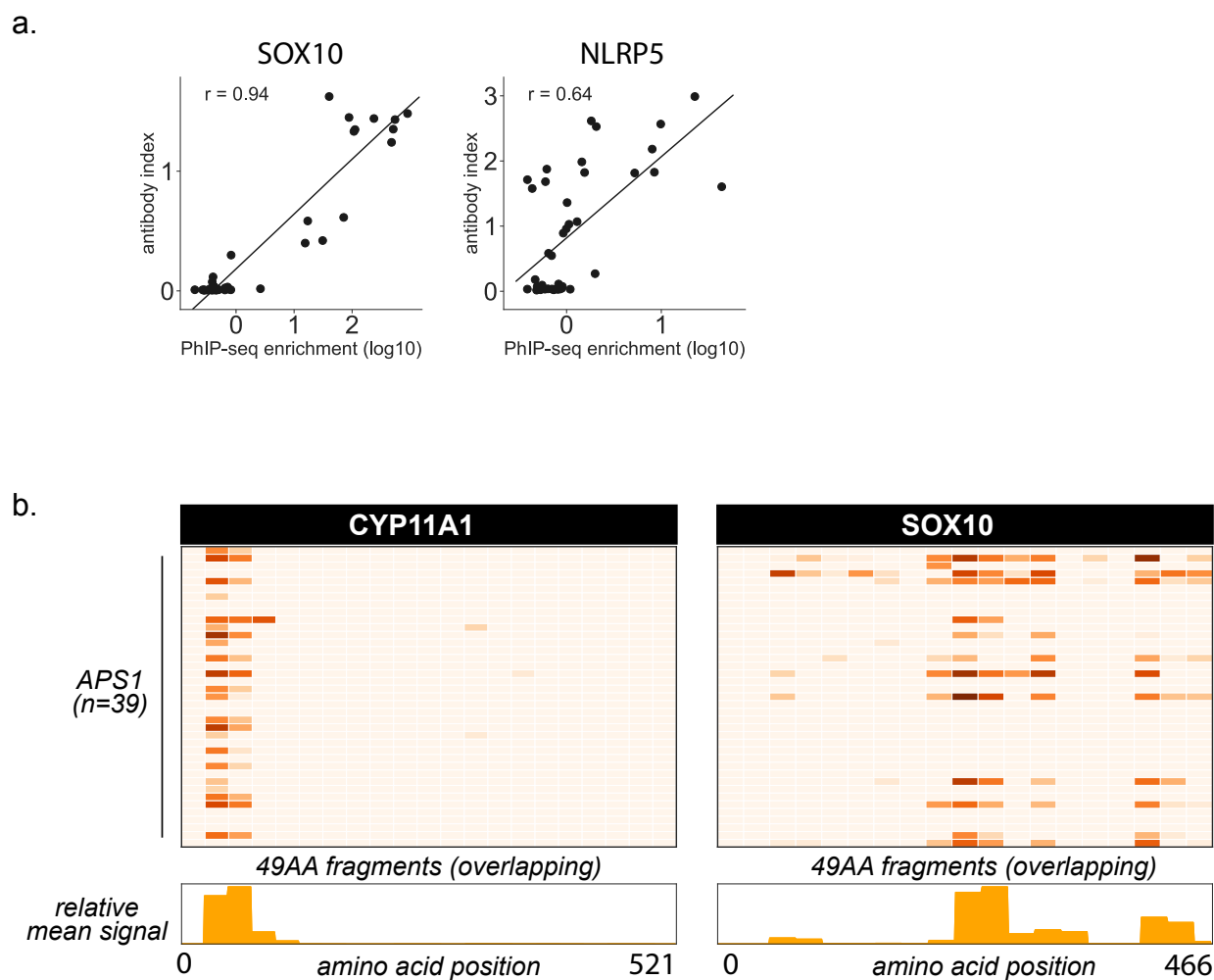
1185 FIGURE SUPPLEMENTS

literature-reported antigens

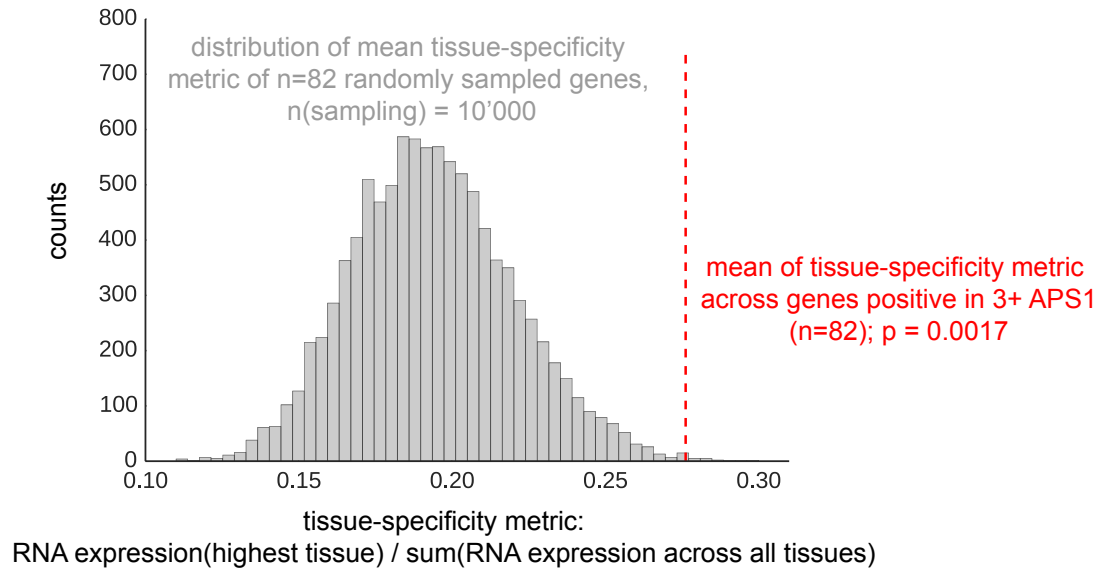


1186 **Figure 1: Figure Supplement 1.** Hierarchically clustered (Pearson) Z-scored heatmap of literature
1187 reported autoantigens that did not meet the cutoff of 10-fold or greater signal over mock-IP in at
1188 least 2/39 APS1 sera and in 0/28 non-APS1 control sera.
1189

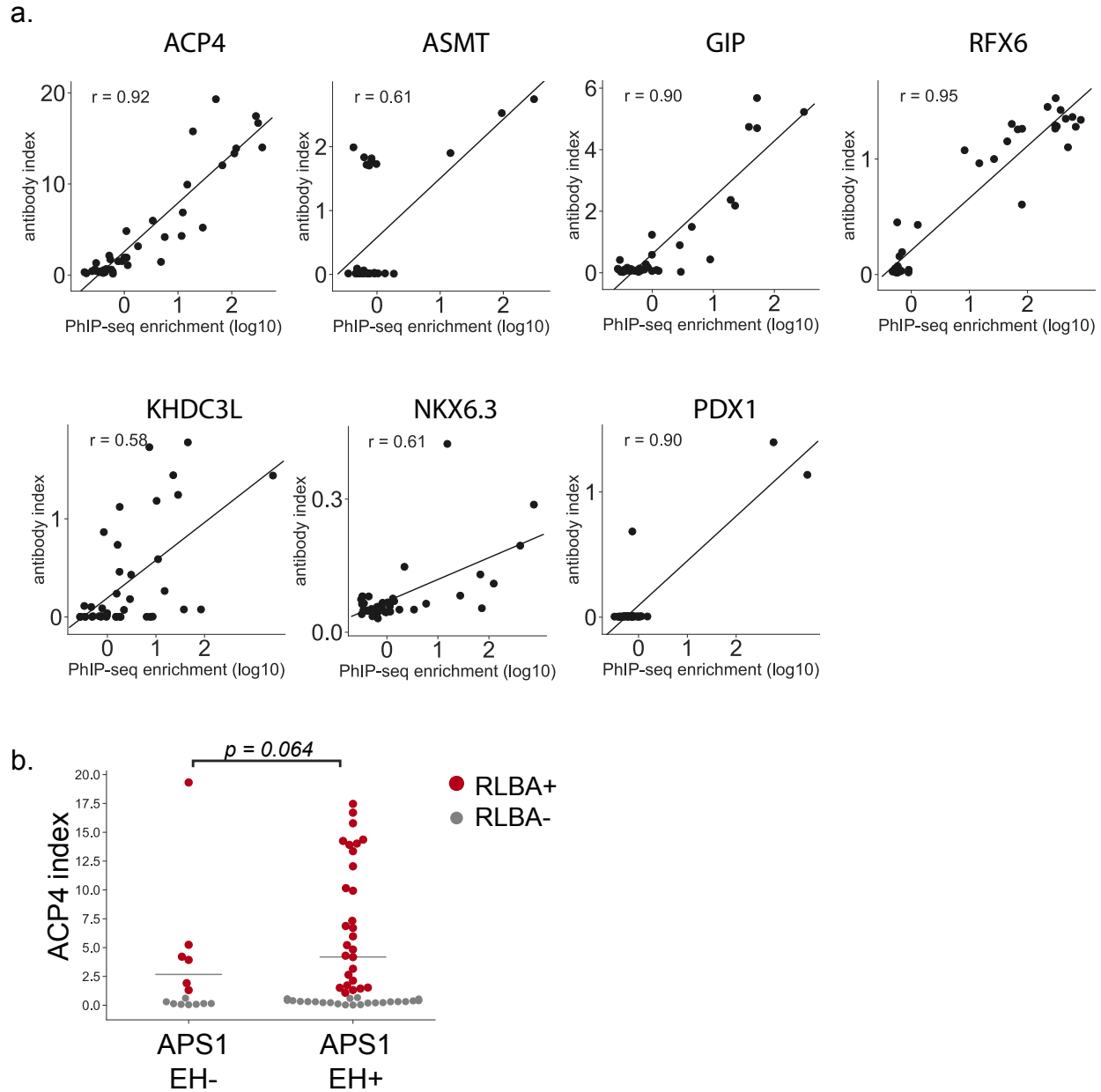
1190



1191 **Figure 1: Figure Supplement 2. A.** Scatterplot of individual PhIP-Seq enrichment values (log10)
1192 over mock-IP as compared to radioligand binding assay antibody index values (1 = commercial
1193 antibody signal) for known antigens SOX10 and NLRP5, with Pearson correlation coefficient r .
1194 **B.** PhIP-Seq enables 49 amino acid resolution of antibody signal from APS1 sera to literature-
1195 reported antigens CYP11A1 and SOX10. Top panels: PhIP-Seq signal (fold-change of each
1196 peptide as compared to signal from mock-IP, log10-scaled) for fragments 1-21 for CYP11A1 and
1197 fragments 1-19 for SOX10. Bottom panels: Trace of normalized signal for CYP11A1 and SOX10
1198 fragments across the mean of all 39 APS1 sera.
1199

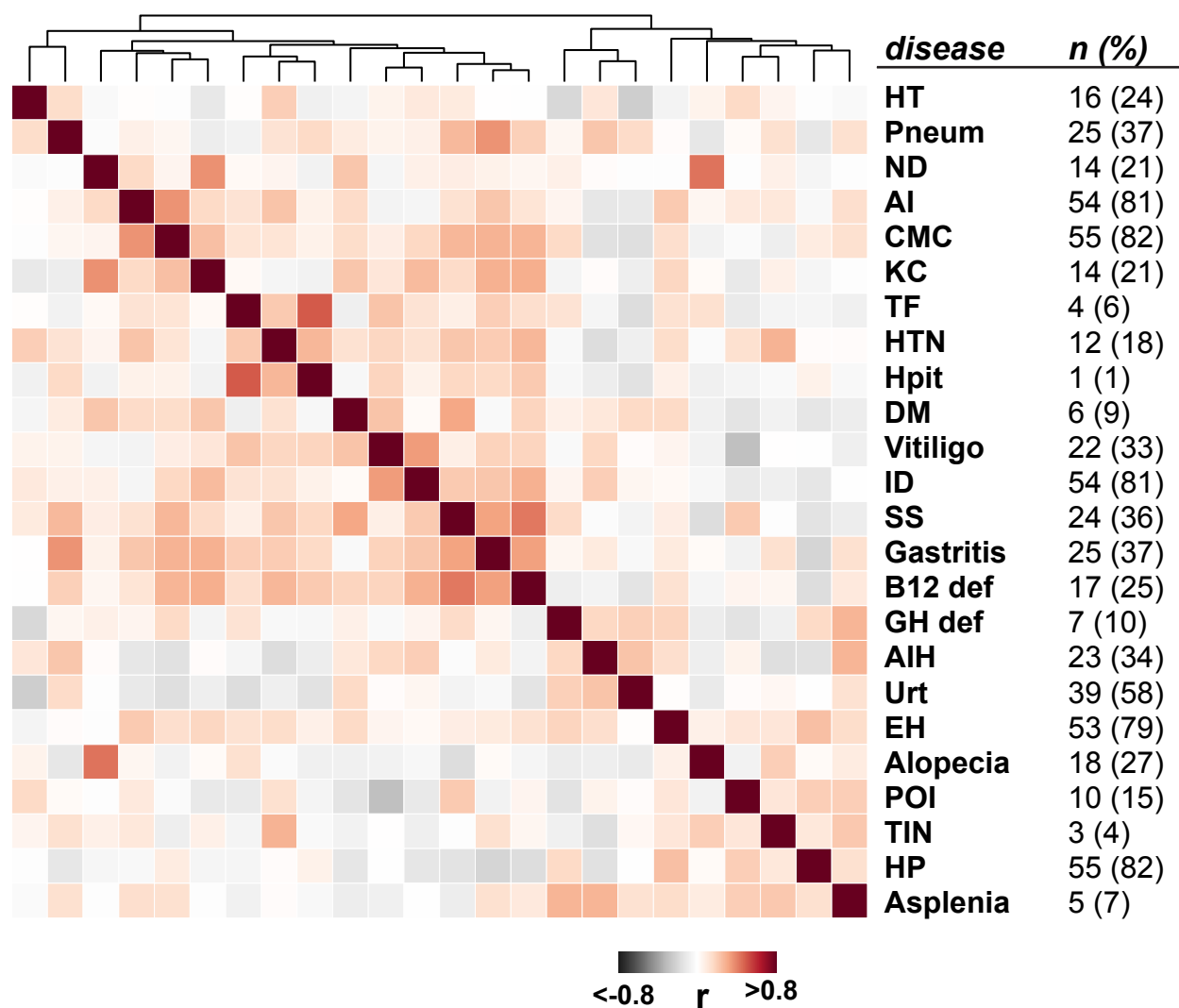


1200
1201 **Figure 2: Figure Supplement 1.** The mean of tissue-specificity ratio of 82 PhIP-Seq antigens
1202 (Figure 2) is increased as compared to the tissue-specificity ratio of n=82 randomly sampled genes
1203 (n-sampling = 10'000). Data from Protein Atlas, HPA/Gtex/Fantom5 RNA consensus dataset
1204 (Uhlen et al., 2015).
1205

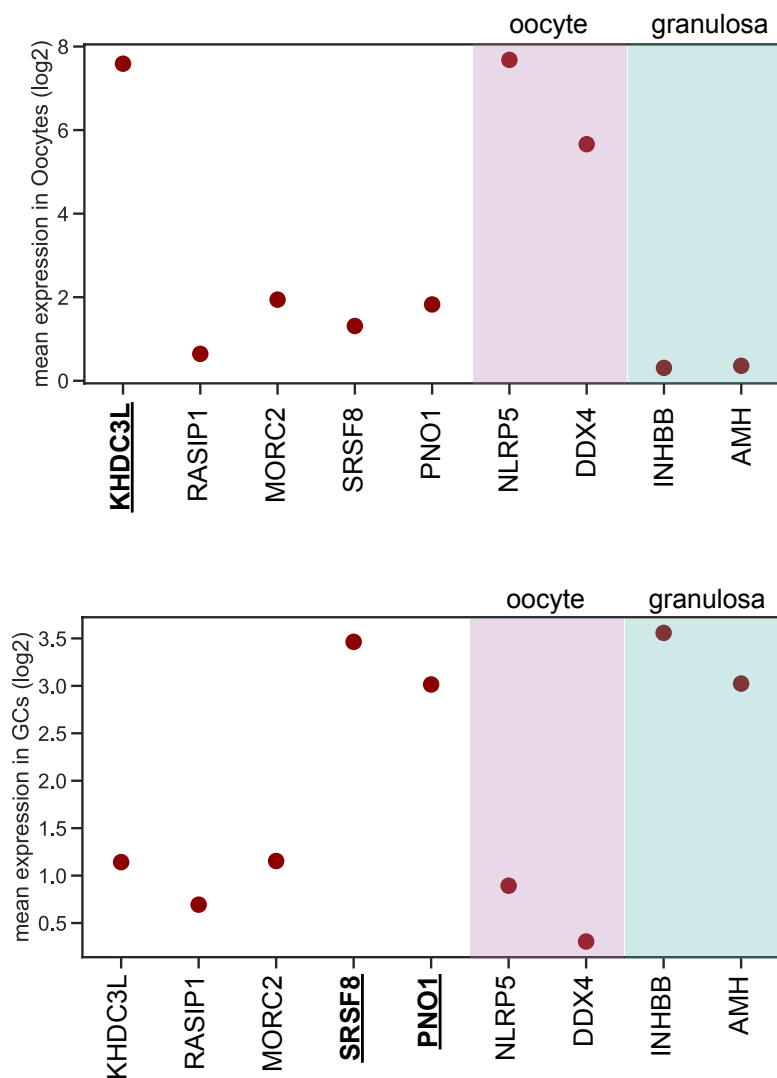


1206
1207
1208
1209
1210
1211
1212
1213

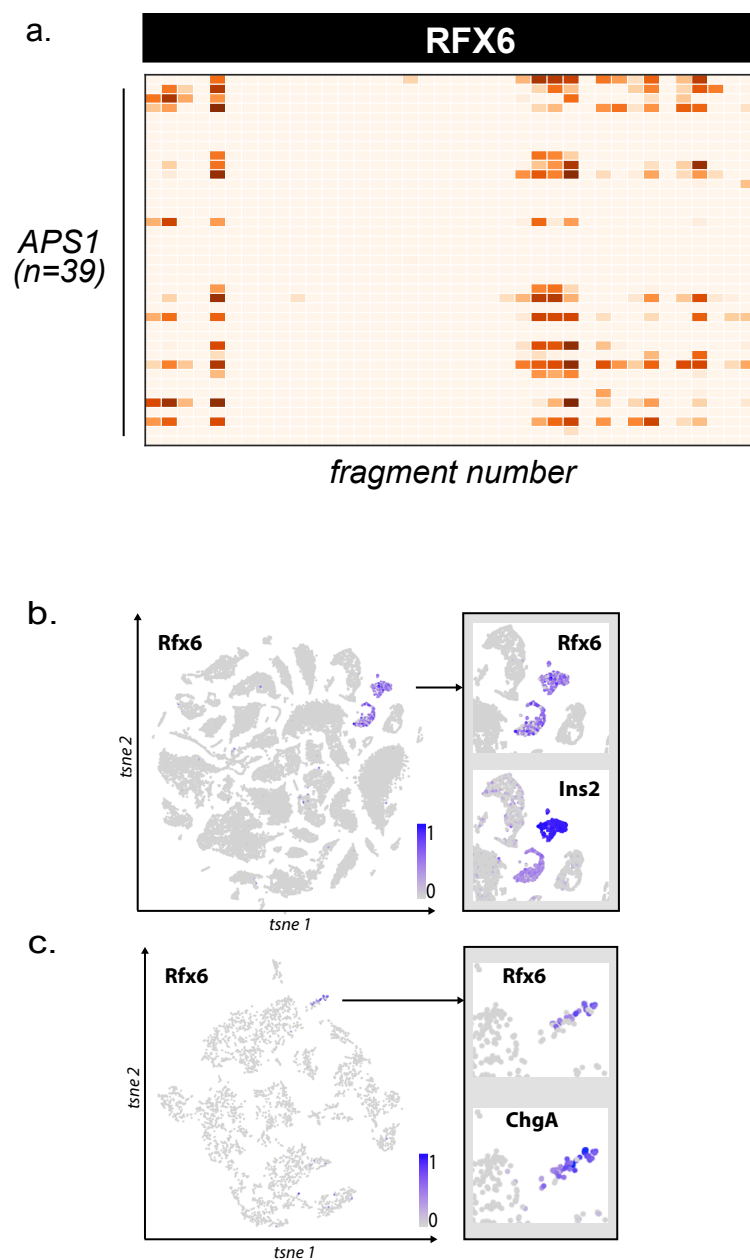
Figure 3: Figure Supplement 1. A. Scatterplot of individual PhIP-Seq enrichment values (log10) over mock-IP as compared to radioligand binding assay antibody index values (1 = commercial antibody signal) for novel antigens ACP4, ASMT, GIP, RFX6, KHDC3L, NKX6.3, and PDX1, with Pearson correlation coefficient r (Note that for PDX1, there are insufficient positive data points for the correlation to be meaningful). **B.** ACP4 RLBA autoantibody index, broken down by enamel hypoplasia (EH) status.



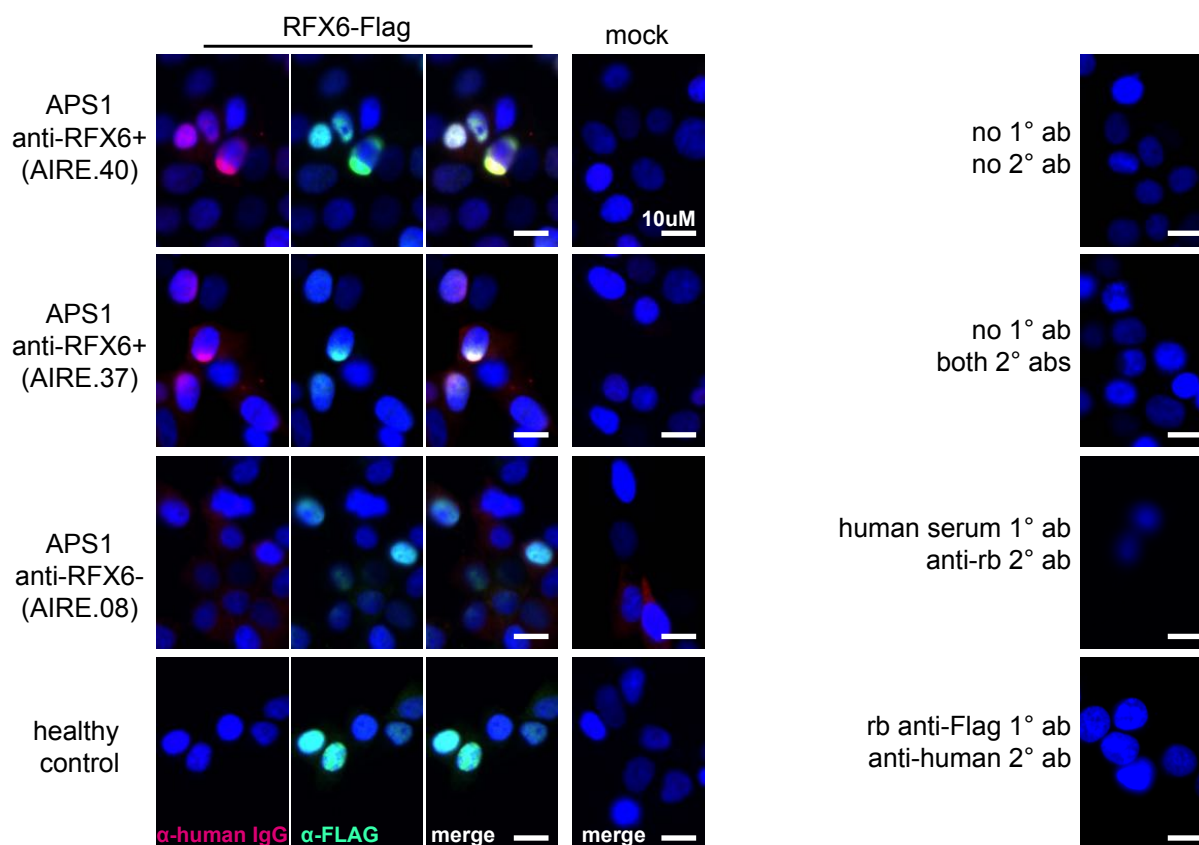
1214 **Figure 4: Figure Supplement 1.** Clustered disease correlations in the APS1
1215 cohort (Spearman's rank correlation; n = 67).
1216



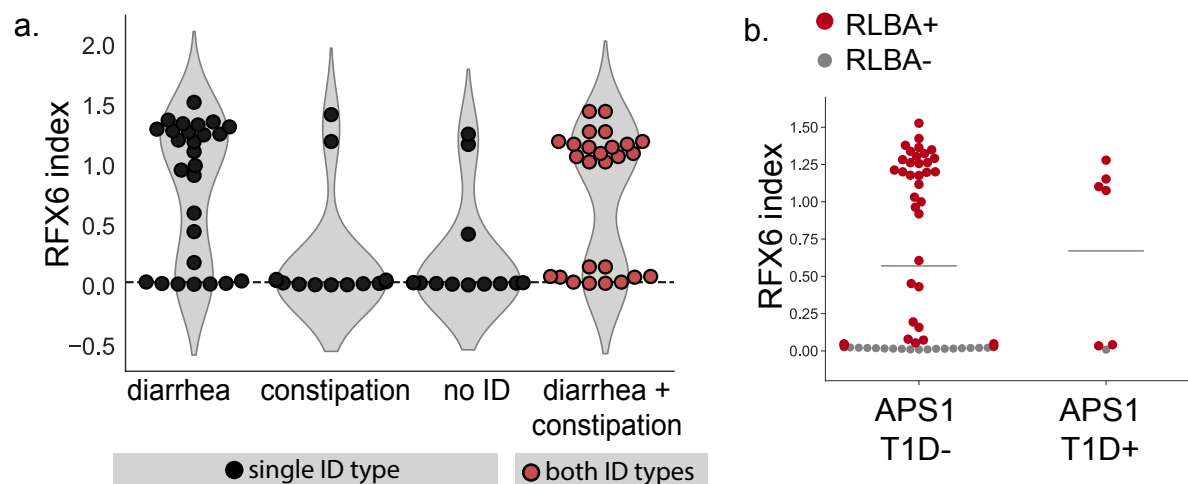
1217
1218 **Figure 4: Figure Supplement 2.** KHDC3L is highly expressed in oocytes (top), but not in
1219 granulosa cells (bottom). In contrast, SRSF8 and PNO1 are highly expressed in granulosa cells,
1220 but not in oocytes. Data from (Y. Zhang et al., 2018)
1221



1222 **Figure 6: Figure Supplement 1. A.** PhIP-Seq enables 49 amino acid resolution of antibody signal
1223 from novel autoantigen RFX6. PhIP-Seq signal (fold-change of each peptide as compared to signal
1224 from mock-IP, log₁₀-scaled) for fragments 1-38 for RFX6 from APS1 sera (n=39). **B.** Single cell
1225 RNA expression of Rfx6. Left: normalized RNA expression of Rfx6 in single cells from 20
1226 different organs. Right inset: Rfx6 shares an expression pattern with pancreatic beta-cell marker
1227 Ins2 (Schaum et al., 2018). **C.** Single cell RNA expression of Rfx6. Left: normalized RNA
1228 expression of Rfx6 in single cells from the intestine. Right inset: Rfx6 shares an expression pattern
1229 with intestinal enteroendocrine cell marker ChgA (Schaum et al., 2018).
1230



1231 **Figure 6: Figure Supplement 2.** Anti-RFX6+ sera (top two panels), but not anti-RFX6- serum or
1232 non-APS1 control serum (bottom two panels), co-stain HEK293T cells transfected with an RFX6-
1233 expressing plasmid. None of the sera tested stain 293T cells transfected with empty vector
1234 ('mock'). No cross-reactivity of secondary antibodies was observed (right panel).
1235



1236 **Figure 6: Figure Supplement 3. A.** APS1 patients with the diarrheal subtype, as well as those
1237 with both subtypes of ID (red), have increased anti-RFX6 antibody signal by RLBA as compared
1238 to those with constipation-type ID or no ID. B. 6/7 (6 diagnosed prior to serum draw, 1 diagnosed
1239 post serum draw) APS1 patients with type 1 diabetes have positive anti-RFX6 signal by RLBA.
1240